Wilfrid Laurier University

Scholars Commons @ Laurier

Theses and Dissertations (Comprehensive)

2016

EPR Paradox, Nonlocality, and Entanglement in Multi-qubit Systems

Raja Emlik
emli2450@mylaurier.ca

Follow this and additional works at: https://scholars.wlu.ca/etd

Part of the Quantum Physics Commons

Recommended Citation

EPR Paradox, Nonlocality, and Entanglement in Multi-qubit Systems

By

Raja Muftah Emlik

ID No. 145822450

Supervisor: Dr. Shohini Ghose

Associate Professor

Department of Physics and Computer Science

A Dissertation Submitted in Partial Fulfilment of the Requirements for the Degree of
Master of Science in Mathematics

Department of Mathematics

Wilfrid Laurier University, Waterloo, Ontario, Canada

Summer 2016

Abstract

Bell inequalities were formulated by John Bell to test the possible violation of local realistic theories by quantum mechanical systems. It was shown that entangled quantum states of multiple particles violate various Bell's inequalities. This proved that quantum mechanics allows correlations between spatially separated systems that have no classical analogue. The main focus of this work is to investigate genuine multiqubit non-locality in families of entangled 3 and 4-qubit pure states by studying a Bell-type inequality that is violated only if all qubits are non-locally correlated. We numerically study the relationship between entanglement and violation of the Svetlichny Bell-type inequality. We analyze non-local correlations in 3-qubit generalized Greenberger-Horne-Zeilinger (GHZ) states, maximal slice (MS) states, and W states. Our studies show that the correlations exhibited by three particles cannot in general be described by hidden variable theories with at most two-particle non-locality. However, some 3-qubit entangled states do not violate the Svetlichny's inequality. We then extend our analysis to 4-qubit generalized Greenberger-Horne-Zeilinger (GHZ) states, maximal slice (MS) states, and W states. The results are similar to the 3-qubit case for GHZ and MS states. The range of parameters for which we see a violation is the same for the 3 and 4-qubit GHZ states. However, the 4-qubit W states do not violate Bell-type inequality, unlike the 3-qubit W states. Our results show the complex nature of multiqubit entanglement and non-locality and provide tools for designing useful quantum communication tasks.

Acknowledgement

I would like to thank my supervisor Professor Shohini Ghose who always offered her time and patience, no matter how busy she was. I owe my deepest gratitude to her for her excellent guidance throughout my thesis. Without her, this work would not have been possible.

My very special thanks go to my family who are waiting for me to go back home with a high degree of education, as without their love, supports, and encouragement, I could not move forward.

Finally, big thanks go to my special family, and particularly to my husband Abdul-hamid for his constant love and support all the time.

Author's Declaration

I declare that the work in this dissertation is original except where indicated by special reference in the text.

No other person's work has been used without due acknowledgement in the main text of the thesis.

It has not been submitted for the consideration of any other degree or diploma in any other tertiary institution.

Raja Muftah Emlik

Contents

List of Figures

List of Abbreviations

Abbreviations	Description
Qubit	Quantum bit.
EPR	Einstein, Podolsky and Rosen.
CHSH	Clauser, Horne, Shimony, and Holt.
GHZ	Greenberger -Horne-Zeilinger.
MS	Maximal slice.
SI	Svetlichny's Inequality.
M_4	4-qubit Bell-type operator.
$|\psi\rangle$	Vector. Also known as a *ket*.
$\langle\psi|$	Vector dual to $|\psi\rangle$. Also known as a *bra*.
$|\psi_A\rangle \otimes |\psi_B\rangle$	Tensor product of $|\psi_A\rangle$ and $|\psi_B\rangle$.
$\langle\psi|QS|\psi\rangle$	Inner product between $\langle\psi|$ and $QS|\psi\rangle$.
$\langle\psi_A|\psi_B\rangle$	Inner product between the vectors $|\psi_A\rangle$ and $|\psi_B\rangle$.
$\langle\ \rangle$	Expectation or average value.
2D	Two dimensional.
3D	Three dimensional.
4D	Four dimensional.

Chapter 1

Introduction

Quantum mechanics is the fundamental theory describing natural phenomena. In fact, phenomena which occur on a very small level (atomic and subatomic) cannot be explained outside the framework of quantum mechanics. In the twentieth century and later, quantum mechanics has been widely studied theoretically and experimentally. It has been successfully applied to many problems including atomic emission [1], particle scattering [2, 3], and radiation-matter interaction [3, 4]. Furthermore, it is now being used as a platform to build the technology of the future such as quantum computers and quantum cryptographic systems. However, the theory remains counterintuitive and puzzling.

The first strong criticism of quantum theory was made by Einstein, Podolsky and Rosen's (EPR) in their 1935 paper entitled "Can quantum mechanical description of physical reality be considered complete?" [5]. They demonstrated what they felt was a lack of completeness in quantum mechanics. They came to this conclusion based on a paradox that they described in the paper, which arose from the fact that according to quantum mechanics, measurements of one member of an entangled pair of objects seem to instantaneously affect the other member, no matter how far away [6].

In order to explain this "spooky action at a distance", Einstein and his colleagues argued that some hidden variable must somehow affect the states of both particles. Also, Einstein was not able to accept that nature expresses itself in a probabilistic way, so this led him to make his famous quote "God does not play dice". Thus, Einstein and

his colleagues concluded that there must be a more complete description of physical reality involving some hidden variables that can characterize the state of affairs in the world in a more causal and deterministic way than the quantum mechanical state [5, 7].

However, in 1964, John Bell designed a test known as Bell's inequality which uses basic assumptions about local realism in order to see if Einstein's conclusions were right or wrong [8, 9]. Bell's calculations proved that local realism conflicted with the predictions of quantum mechanics. He showed that quantum mechanics cannot be both local and realistic. In other words, quantum mechanics violates Bell's inequality, and it has been widely accepted as a non-local theory. This paradox in fact has been confirmed by several laboratory experiments since the 1970s [8, 10].

1.1   Motivation

The heart of quantum mechanics is entanglement or quantum correlations, which have been observed in numerous experiments. There has been a great deal of investigation of bipartite quantum correlations using different tools such as different forms of Bell-type inequalities and non-locality witnesses [11]. However, even though many studies have been conducted, a comprehensive understanding of multipartite quantum correlations has not yet been achieved because of the exponential growth in the complexity of the problem as we increase the number of correlated quantum particles [12]. In the present work, we aim to address the open question of characterizing multipartite quantum correlations by exploring the violation of Bell inequalities. Our goal is to investigate genuine multiparty correlations in an n-party quantum system when all of the spatially separated parties forming the system are quantum correlated. Svetlichny laid the cornerstone in the study of genuine multiparty non-locality by designing a new inequality known as Svetlichny's inequality [13].

1.2   Thesis Organization

The thesis begins with an overview and introduction of the basic concepts (chapter 2). The next chapter (chapter 3) discusses bipartite entanglement and the EPR paradox. In addition, we show how quantum mechanics predicts a violation of the Bell inequality. Chapter 4 presents our investigation of genuine 3-qubit entangled (GHZ, MS, and W) states by analyzing a Bell-type inequality (Svetlichny's inequality). Numerical calculations and plots show our investigation of the relationship between entanglement and violation of the Svetlichny Bell-type inequality. In chapter 5, we extend our analysis to 4-qubit states by following similar steps as in chapter 4. This includes our new and surprising results related to the quantum correlations in 4-qubit W states. Finally, in Chapter 6, we summarize the work and provide an outlook.

Chapter 2

Background

In this chapter, we introduce some background about qubits in order to explain the basic ideas that are of importance for the subject we are treating here.

2.1 Qubit

A quantum bit, or qubit for short, is the fundamental building block of quantum information. It is the quantum analogue to the term bit in information theory [14]. A qubit has two states 0 and 1 in contrast to the classical bit that can be either 0 or 1. According to the superposition principle [14], a qubit can be prepared in any superposition state of the form:

$$|\psi\rangle = \alpha|0\rangle + \beta|1\rangle, \text{ and } \alpha^2 + \beta^2 = 1. \tag{2.1}$$

where α and β are complex numbers, and the notation $|\ \rangle$ is called Dirac notation that is the standard notation for states in quantum mechanics. The special states $|0\rangle$ and $|1\rangle$ are known as computational basis states, and form an orthonormal basis for this vector space as:

$$|0\rangle = \begin{pmatrix} 1 \\ 0 \end{pmatrix}, \quad |1\rangle = \begin{pmatrix} 0 \\ 1 \end{pmatrix}. \tag{2.2}$$

In order to know the actual value of the qubit, we must make a measurement. Measuring $|\psi\rangle$ in the $\{|0\rangle, |1\rangle\}$ basis yields $|0\rangle$ with probability $|\alpha|^2$, and $|1\rangle$ with probability $|\beta|^2$. In addition, one important aspect of the measurement process is that it collapses the state of the qubit [15]. For example, if the outcome of the measurement of (2.1) yields $|0\rangle$, then following the measurement, the qubit is in state $|0\rangle$. This means that

we cannot gather any additional information about α, β by repeating the measurement [14, 15].

The qubit states can be visualized using a Bloch sphere as indicated in figure 2.1. North and south poles correspond respectively to $|0\rangle$ and $|1\rangle$ and more generally, opposite points represent mutually orthogonal states [16]. Thus, we can rewrite (2.1) as:

$$|\psi\rangle = \cos\left(\frac{\theta}{2}\right)|0\rangle + e^{i\varphi}\sin\left(\frac{\theta}{2}\right)|1\rangle, \tag{2.3}$$

with $\theta \in [0, \pi]$ and $\varphi \in [0, 2\pi]$.
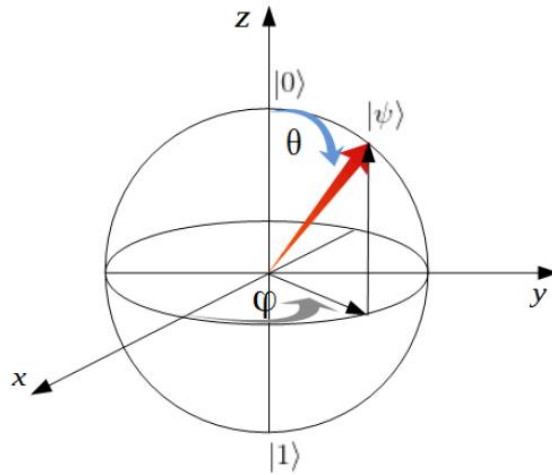
Figure 2.1: Bloch sphere representation of a qubit.

Furthermore, any possible manipulation of (2.2) can be represented with a 2 by 2 matrix. We can further say that this matrix must be Hermitian ($i.g\ \hat{O} = \hat{O}^\dagger$) due to the constraints of quantum mechanics [15]. This matrix $\hat{O}$ can be written as a sum of Pauli matrices, which are given by:

$$\sigma_i = I = \begin{pmatrix} 1 & 0 \\ 0 & 1 \end{pmatrix}, \sigma_x = \begin{pmatrix} 0 & 1 \\ 1 & 0 \end{pmatrix}, \sigma_y = \begin{pmatrix} 0 & -i \\ i & 0 \end{pmatrix}, \sigma_z = \begin{pmatrix} 1 & 0 \\ 0 & -1 \end{pmatrix}.$$

where σ_i does nothing, σ_x gate maps $|0\rangle$ to $|1\rangle$ and $|1\rangle$ to $|0\rangle$, σ_z leaves the basis state $|0\rangle$ unchanged and maps $|1\rangle$ to $-|1\rangle$, and σ_y does both. They obey the relationship $\sigma_j^2 = I$ and the anti-commutator $\{\sigma_j, \sigma_k\} = 2\delta_{jk}I$ for all $\{j, k\} = \{x, y, z, i\}$[16]. δ_{jk} is the usual Kroncecker delta, and I is the 2×2 unit matrix. Hence, we show that:

$$\{\sigma_j, \sigma_k\} = 2\delta_{jk}I,$$

$$\sigma_j\sigma_k + \sigma_k\sigma_j = 2\delta_{jk}I.$$

For example,

$$\sigma_x\sigma_y = \begin{pmatrix} 0 & 1 \\ 1 & 0 \end{pmatrix}\begin{pmatrix} 0 & -i \\ i & 0 \end{pmatrix} = i\sigma_z,$$

$$\sigma_y\sigma_x = \begin{pmatrix} 0 & -i \\ i & 0 \end{pmatrix}\begin{pmatrix} 0 & 1 \\ 1 & 0 \end{pmatrix} = -i\sigma_z.$$

Thus,

$$\sigma_x\sigma_y + \sigma_y\sigma_x = 0.$$

If $j \neq k$, the anti-commutation of different Pauli matrices is zero, so we say Pauli matrices anti-commute with each other [17].

2.2   Two Qubits

A two qubit states has four computational basis states denoted $|00\rangle, |01\rangle, |10\rangle$, and $|11\rangle$. They can be in a superposition of these four states, so the general state of a two qubit system can be written as:

$$|\psi\rangle = \alpha_{00}|00\rangle + \alpha_{01}|01\rangle + \alpha_{10}|10\rangle + \alpha_{11}|11\rangle, \tag{2.3}$$

where $\sum_{ij}|\alpha_{ij}|^2 = 1$.

The two qubit states obey the same rules as single qubit states when they are measured. For instance, when we measure $|\psi\rangle$ in (2.3), the probability that the first qubit is in state i, and the second qubit is in state j is $P(i, j) = |\alpha_{ij}|^2$ [14]. Following the measurement, the state of the two qubits is $|\psi'\rangle = |ij\rangle$. Measuring the first qubit alone gives 0 with probability $|\alpha_{00}|^2 + |\alpha_{01}|^2$ leaving the post-measurement state:

$$|\psi'\rangle = \frac{\alpha_{00}|00\rangle + \alpha_{01}|01\rangle}{\sqrt{|\alpha_{00}|^2 + |\alpha_{01}|^2}}. \tag{2.4}$$

which is renormalized by the factor $\sqrt{|\alpha_{00}|^2 + |\alpha_{01}|^2}$. This means therefore it still satisfies the normalization condition [15].

2.3   Entanglement

Entanglement is a quantum mechanical phenomenon in which the quantum states of two or more objects have to be described with reference to each other even though the individual objects may be spatially separated. An entangled state cannot be written as a tensor product or separable state, for example, $|\psi_{AB}\rangle \neq |\psi_A\rangle \otimes |\psi_B\rangle$ [15]. Measurements performed on one system seem to be instantaneously effecting other systems entangled with it. For instance, the state of a two qubit system given by $|\psi\rangle = \frac{1}{\sqrt{2}}(|00\rangle + |11\rangle)$, called the Bell state, cannot be represented as $(\alpha_0|0\rangle + \alpha_1|1\rangle) \otimes (\beta_0|0\rangle + \beta_1|1\rangle)$ as we mentioned above.

We cannot precisely specify the state of each individual qubit in this system because the states of the two qubits are entangled. If the first qubit (or the second qubit) is measured then the outcome is 0 with probability $1/2$ and 1 with probability $1/2$ [14, 16]. However, if the outcome of the first qubit is 0, then a measurement of the second qubit results in 0 with certainty and vice versa. This is true no matter how large the spatial separation between the two particles. We can also construct a Bell basis with the addition of the states:

$$|\psi\rangle = \frac{1}{\sqrt{2}}(|00\rangle - |11\rangle),$$

$$|\psi\rangle = \frac{1}{\sqrt{2}}(|01\rangle + |10\rangle),$$

$$|\psi\rangle = \frac{1}{\sqrt{2}}(|01\rangle - |10\rangle).$$

Each of these states is maximally entangled, and mutually orthogonal [16].

For three and four qubits, there are different classes of entanglement such as GHZ, MS, and W states. These states are studied in the fourth and fifth chapters.

Chapter 3

Two Qubit Entanglement

3.1 EPR Paradox

The EPR paradox, named after Albert Einstein, Boris Podolsky and Nathan Rosen, was a thought experiment which revealed what later would be called entanglement [5]. The EPR paper presented an argument to show that quantum mechanics was an incomplete description of nature as follows:

3.1.1 The EPR Argument

The EPR argument was based on certain assumptions about the meaning of reality and locality. The first assumption is locality, which states that the results of measurements performed on one particle must be independent of whatever is done at the same time to its entangled particle located at an arbitrary distance away. The second assumption is realism, which states that the outcome of a measurement on one of the particles reflects properties with definite values (element of reality) that the particle carried prior to and independent of the measurement. Given these seemingly reasonable assumptions, EPR asserted that any complete physical theory must be able to predict the values of all elements of reality (called by them "condition of completeness") [5].

The EPR description involves two particles A and B that interacted at some moment in the past and then flew far apart (Figure 3.1, p. 10). The distance is so large after the separation that there is no more interaction between the particles. According to the locality assumption, measurements made by Alice on particle A cannot instantaneously

9

influence the measurement outcomes of particle B during the experiment and vice versa. If Alice measures the position of particle A to be x, she can predict with certainty without disturbing particle B that the location of particle B is $x - x_0$ [18].

Hence, in accordance with the reality assumption, the position of particle B is an element of reality. Alternatively, if Alice measures the momentum of particle A to be p, she can predict with certainty without disturbing particle B, that the momentum of particle B is $-p$ which means there is also an element of reality in accordance with the second assumption.
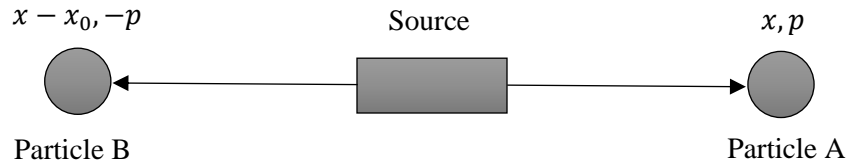
Figure 3.1: Set-up for the EPR thought experiment.

However, this case conflicts with quantum mechanics according to the uncertainty principle, which states that we cannot predict with certainty the values of both position and momentum at the same time [19]. Indeed, quantum mechanics describes the perfect correlation of entangled particles between their positions and momenta. For instance, it allows Alice to make precise predictions about the position and momentum of particle B just by measuring particle A. This seems to violate local realism since the first measurement affects a property of a physical object that can be far away from where the measurement took place. Consequently, Einstein and his co-authors summarized in their original paper that quantum mechanics must be an incomplete theory [5, 15, 18].

3.2   Bell's Inequality

Bell's inequality is the most famous and important contribution to the discussion of the validity of local realism in quantum mechanics. The goal of Bell's inequality is to test whether the assumptions of local realism are indeed compatible with the outcomes of measurements of entangled particles in a real experimental setting [8, 9].

Bell proposed the following test: Consider a source that emits two entangled particles in opposite directions. One particle goes toward Alice and the other particle goes toward Bob. In addition, both have two different measurement devices, such that the measurements' outcomes of each device are +1 or −1. Alice measures the particle she receives, and she chooses to do one of two different measurements at random. Then, based on her measurement, she has an outcome which is labelled $Q = +1$ or −1 or an outcome $R = +1$ or −1 [18, 15].

Likewise, Bob measures randomly one of two variables S or T, each taking value +1 or −1. The time of the experiment is the same for Alice and Bob, so Alice's measurement cannot disturb the result of Bob's measurement and vice versa according to EPR's assumptions. Below is some simple algebra with the quantity:

$$QS + RS + RT - QT = (Q + R)S + (R - Q)T = \pm 2. \tag{3.1}$$

Repeating the experiment over many trials, we can calculate the average value of the quantities QS, RS, RT and QT, denoted by $\langle QS \rangle, \langle RS \rangle, \langle RT \rangle$ and $\langle QT \rangle$. Before measurements have happened, the probability of getting the values $Q = q, R = r, S = s, T = t$ is $p(q, r, s, t)$, then the average is:

$$\langle QS \rangle + \langle RS \rangle + \langle RT \rangle - \langle QT \rangle = \sum_{qrst} p(q, r, s, t)(qs + rs + rt - qt) \tag{3.2}$$

$$\leq \sum_{qrst} p(q, r, s, t) \times 2 \tag{3.3}$$

$$= 2 . \tag{3.4}$$

Thus, we obtain Bell's inequality:

$$\langle QS \rangle + \langle RS \rangle + \langle RT \rangle - \langle QT \rangle \leq 2. \tag{3.5}$$

Bell's inequality must exist between 2 and -2. This version is known as the CHSH inequality, named after the initials of the authors that discovered this form of Bell's inequality. For a pair of entangled qubits, the Bell-CHSH inequality is:

$$CHSH = |\langle AB + AB' + A'B - A'B' \rangle|, \tag{3.6}$$

where A and A' denote measurements of qubit 1 by Alice in two different randomly chosen directions. Similarly B and B' label the measurements of qubit 2 by Bob along different directions [18].

Now let's apply quantum mechanics to the inequality. It is possible for each particle to be in a superposition of 0 and 1. Given a quantum system of two qubits, we can for example, write the joint quantum state as:

$$|\psi\rangle = \frac{|01\rangle - |10\rangle}{\sqrt{2}}. \tag{3.7}$$

This is called a Bell state or an EPR pair as introduced in chapter 2.

Let us assume that the first qubit goes to Alice, and the second qubit goes to Bob. Each performs the measurements by applying the following observables:

$$Q = Z_1, \quad S = \frac{-Z_2 - X_2}{\sqrt{2}}, \tag{3.8}$$

$$R = X_1, \quad T = \frac{Z_2 - X_2}{\sqrt{2}}, \tag{3.9}$$

where $Z = \begin{pmatrix} 1 & 0 \\ 0 & -1 \end{pmatrix}$ and $X = \begin{pmatrix} 0 & 1 \\ 1 & 0 \end{pmatrix}$ are Pauli matrices. The indices 1 and 2 refer to the first qubit and the second qubit respectively. By doing simple calculations to calculate $\langle QS \rangle, \langle RS \rangle, \langle RT \rangle$ and $\langle QT \rangle$, we have:

$$\langle QS \rangle = \langle \psi | QS | \psi \rangle,$$

$$\langle QS \rangle = \langle \psi | Z_1 \left(\frac{-Z_2 - X_2}{\sqrt{2}} \right) | \psi \rangle,$$

$$\langle QS \rangle = \left(\frac{\langle 01| - \langle 10|}{\sqrt{2}} \right) \left(\frac{-Z_1 Z_2}{\sqrt{2}} \right) \left(\frac{|01\rangle - |10\rangle}{\sqrt{2}} \right)$$

$$+ \left(\frac{\langle 01| - \langle 10|}{\sqrt{2}} \right) \left(\frac{-Z_1 X_2}{\sqrt{2}} \right) \left(\frac{|01\rangle - |10\rangle}{\sqrt{2}} \right),$$

$$\langle QS \rangle = \frac{1}{2\sqrt{2}} \begin{bmatrix} (\langle 01| - \langle 10|)((-Z_1 Z_2)|01\rangle - (-Z_1 Z_2)|10\rangle) + \\ (\langle 01| - \langle 10|)((-Z_1 X_2)|01\rangle - (-Z_1 X_2)|10\rangle) \end{bmatrix},$$

with

$$X|0\rangle = |1\rangle,$$
$$X|1\rangle = |0\rangle,$$

and

$$Z|0\rangle = |0\rangle,$$
$$Z|1\rangle = -|1\rangle.$$

Hence,

$$\langle QS \rangle = \frac{1}{2\sqrt{2}} [(\langle 01| - \langle 10|)(|01\rangle - |10\rangle) - (\langle 01| - \langle 10|)(|00\rangle + |11\rangle)],$$

$$\langle QS \rangle = \frac{1}{2\sqrt{2}} [\langle 01|01\rangle - \langle 10|01\rangle - \langle 01|10\rangle + \langle 10|10\rangle - \langle 01|00\rangle + \langle 10|00\rangle$$

$$- \langle 01|11\rangle + \langle 10|11\rangle],$$

where

$$\langle 01|01\rangle = \langle 10|10\rangle = 1,$$

$$\langle 10|01\rangle = \langle 01|10\rangle = \langle 01|00\rangle = \langle 10|00\rangle = \langle 01|11\rangle = \langle 10|11\rangle = 0.$$

Thus,

$$\langle QS \rangle = \frac{1}{2\sqrt{2}} [\langle 01|01 \rangle + \langle 10|10 \rangle] = \frac{1}{\sqrt{2}}.$$

Similarly, for the other terms, we obtain:

$$\langle RS \rangle = \langle RT \rangle = 1/\sqrt{2}, \text{ and } \langle QT \rangle = -1/\sqrt{2}. \tag{3.10}$$

By substituting these values in (3.5), we have:

$$\langle QS \rangle + \langle RS \rangle + \langle RT \rangle - \langle QT \rangle = 4/\sqrt{2} = 2\sqrt{2}. \tag{3.11}$$

As a result, quantum mechanics violates Bell's inequality (3.5), and we can infer that one of the EPR's assumptions is false. Therefore, quantum mechanics is not locally realistic. Furthermore, experimental results are consistent with quantum mechanical predictions and inconsistent with local realism theories [8, 15, 19]. All experimental tests thus far have confirmed that quantum entanglement leads to a violation of a Bell-type inequality [20, 21, 22, 23, 24, 25, 26, 27, 28, 29].

Chapter 4

Three Qubit Entanglement

Violations of Bell's inequality by two-qubit entangled states have been demonstrated both in theory and in experiments. Unlike the two-qubit case, where all maximally entangled two-qubit states are equivalent up to local changes of basis, three qubits can be entangled in fundamentally different ways [30]. Here, we use Svetlichny's inequality, described in the next paragraph, to measure the genuine non-locality of 3-qubit states.

Svetlichny's inequality (SI) is considered to be the best Bell-type inequality to identify genuine non-locality of pure tripartite entangled states. It can distinguish between 2-qubit versus genuine 3-qubit non-locality [31]. Derivation of SI is similar to Bell-CHSH inequality, but SI consists of three particles rather than two particles to test for genuine tripartite non-locality:

$$S = |\langle ABP + AB'P' + A'BP' - A'B'P' \rangle|, \tag{4.1}$$

where $P = (C + C')$ and $P' = (C - C')$, with C and C' labeling Charlie's local measurements of the third qubit along two different directions. Svetlichny showed that when non-local correlations are allowed between, at most, two of the three qubits, then the function S in (4.1) is always bounded by a value of 4 ($S \leq 4$) [12]. However, a quantum mechanical calculation of the expectation value $\langle \psi | S | \psi \rangle$ shows that this bound of 4 can be violated by pure 3-qubit entangled states for certain choices of measurement directions. Thus, this implies a violation of the assumptions of local realism. In this chapter, we investigate the following 3-qubit entangled states:

GHZ (Greenberger-Horne-Zeilinger) class states

$$|\psi_G\rangle = \alpha|000\rangle + \beta|111\rangle, \quad \alpha^2 + \beta^2 = 1. \tag{4.2}$$

Maximal Slice (MS) states

$$|\psi_{MS}\rangle = \alpha|000\rangle + \beta|110\rangle + \gamma|111\rangle, \quad \alpha^2 + \beta^2 + \gamma^2 = 1. \tag{4.3}$$

and W class states

$$|\psi_W\rangle = \alpha|001\rangle + \beta|010\rangle + \gamma|100\rangle, \quad \alpha^2 + \beta^2 + \gamma^2 = 1. \tag{4.4}$$

where α, β, and γ are real.

By using Pauli matrices $\vec{\sigma}$ and a unit vector $\vec{v}$, we can calculate each term in (4.1) as follows:

$$\langle ABC \rangle = \langle \psi | \vec{a}.\vec{\sigma} \otimes \vec{b}.\vec{\sigma} \otimes \vec{c}.\vec{\sigma} \, |\psi\rangle, \tag{4.5}$$

where

$$\vec{a}.\vec{\sigma} = \begin{bmatrix} a_z & a_x - ia_y \\ a_x + ia_y & -a_z \end{bmatrix}, \quad \vec{b}.\vec{\sigma} = \begin{bmatrix} b_z & b_x - ib_y \\ b_x + ib_y & -b_z \end{bmatrix},$$

and

$$\vec{c}.\vec{\sigma} = \begin{bmatrix} c_z & c_x - ic_y \\ c_x + ic_y & -c_z \end{bmatrix}.$$

Also, $|\psi\rangle$ can be written as a unit vector $\vec{v}$. For example, the unity vector corresponding to (4.2) is:

$$|\psi\rangle = \begin{pmatrix} \alpha \\ 0 \\ 0 \\ 0 \\ 0 \\ 0 \\ 0 \\ \beta \end{pmatrix}, \quad \text{and} \quad \langle\psi| = (\alpha \; 0 \; 0 \; 0 \; 0 \; 0 \; 0 \; \beta). \tag{4.6}$$

We can rewrite (4.5) in terms of the spherical angles $\theta_a, \theta_b, \theta_c$ and $\varphi_a, \varphi_b, \varphi_c$ corresponding to the direction of the measurement unit vector for each qubit with

$$a = (sin\theta_a cos\varphi_a, sin\theta_a sin\varphi_a, cos\theta_a), \tag{4.7}$$

We can similarly convert b and c to spherical coordinates.

Moreover, we must perform a maximization over the 12 angles of all the terms in (4.1) describing the two measurements of each qubit in order to find the maximum value of the Svetlichny function. This maximum can be calculated numerically using an optimization technique [31]. Since our function is a constrained nonlinear multivariable function, we chose the Matlab fmincon solver to seek the minimizer of our function. Fmincon command begins with a variety of initial guesses to search for all the possible optimal points (local and global) and to satisfy the constraints of θ from 0 to π and φ from 0 to 2π.

In order to run our code, we use a loop statement (FOR loop) of the variables as shown in the appendix. The step size in a FOR loop taken as 0.001, and we set up optimization options parameters to allow us to tune or modify the optimization process in order to have an accurate result. To ensure that our result is correct, we developed another code which explicitly calculated the value of the Svetlichny function over a uniform, finely-spaced grid of all possible angles and found the global optimum from the calculated values. This method gave us a similar result to the first method. We also tested both methods by choosing certain values for the variables $\alpha, \beta,$ and γ. The results of the first method were consistent with the results of the second method.

4.1   Generalized GHZ States (GGHZ)

The GGHZ states are:

$$|\psi_G\rangle = \alpha|000\rangle + \beta|111\rangle, \tag{4.8}$$

where the complex parameters $\alpha,$ and β satisfy the normalization condition: $\alpha^2 + \beta^2 = 1$. First we calculate each term in the Svetlichny function. For example,

$$\langle ABC \rangle = (\alpha^2 - \beta^2)cos\theta_a cos\theta_b cos\theta_c +$$

$$2\alpha\beta\ sin\theta_a\ sin\theta_b sin\theta_c\ cos(\varphi_a + \varphi_b + \varphi_c). \tag{4.9}$$

Likewise, we can find an expression for the rest of the terms in (4.1), and therefore by adding them, we rewrite the Svetlichny function as a sum of two terms,

$$S(\psi_G) = |(\alpha^2 - \beta^2)k_1 + 2\alpha\beta k_2|, \tag{4.10}$$

where k_1 and k_2 are the functions of all measurement angles,

$$k_1 = cos\theta_a[cos\theta_b(cos\theta_c + cos\theta_{c'}) + cos\theta_{b'}(cos\theta_c - cos\theta_{c'})] +$$

$$cos\theta_{a'}[cos\theta_b(cos\theta_c - cos\theta_{c'}) - cos\theta_{b'}(cos\theta_c + cos\theta_{c'})], \tag{4.11}$$

$$k_2 = sin\theta_a\big[sin\theta_b\big(sin\theta_c cos(\varphi_a + \varphi_b + \varphi_c) + sin\theta_{c'}cos(\varphi_a + \varphi_b + \varphi_{c'})\big) +$$

$$sin\theta_{b'}\big(sin\theta_c cos(\varphi_a + \varphi_{b'} + \varphi_c) - sin\theta_{c'}cos(\varphi_a + \varphi_{b'} + \varphi_{c'})\big)\big] +$$

$$sin\theta_{a'}\big[sin\theta_b\big(sin\theta_c cos(\varphi_{a'} + \varphi_b + \varphi_c) - sin\theta_{c'}cos(\varphi_{a'} + \varphi_b + \varphi_{c'})\big) -$$

$$sin\theta_{b'}\big(sin\theta_c cos(\varphi_{a'} + \varphi_{b'} + \varphi_c) + sin\theta_{c'}cos(\varphi_{a'} + \varphi_{b'} + \varphi_{c'})\big)\big]. \tag{4.12}$$

The maximum of the function in Equation 4.10 can be found by numerical optimization in Matlab. Figure 4.1 (p. 19) shows that GHZ states have the maximum value of SI which is $4\sqrt{2}$ at $\alpha^2 = \beta^2 = 0.5$. We can calculate β^2 from the normalized condition $\beta^2 = 1 - \alpha^2$. When we plot $S(\psi_G)$ versus β^2, the result is similar to figure 4.1. In addition, it is easy to see the values of α^2 and β^2, labeled by the vertical dashed lines, for which 3-qubit states violate SI. This calculation verifies the calculation that was done in [31].
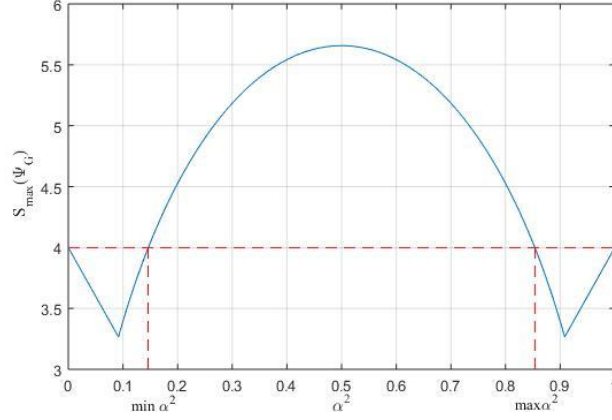
Figure 4.1: $S(\psi_G)$ versus α^2 was numerically verified by (4.10) to show the maximum violateon ($4\sqrt{2}$) of the Svetlichny operator. The horizontal dashed line shows the values of α^2 and β^2 for which the max value is 4 set by (4.1) while the vertical dashed lines display the values of α^2 and β^2 for which the max value is greater than 4.

4.2   Maximal Slice (MS) states

Next, we investigate general MS states that have not been previously analyzed:

$$|\psi_{MS}\rangle = \alpha|000\rangle + \beta|110\rangle + \gamma|111\rangle, \tag{4.13}$$

where the complex parameters $\alpha, \beta,$ and γ satisfy the normalization condition: $\alpha^2 + \beta^2 + \gamma^2 = 1$. We can calculate each term in the Svetlichny function:

$$\langle ABC\rangle = (\alpha^2 + \beta^2 - \gamma^2)cos\theta_a cos\theta_b cos\theta_c +$$

$$2\alpha\beta sin\theta_a sin\theta_b cos\theta_c cos(\varphi_a + \varphi_b) +$$

$$2\alpha\gamma sin\theta_a \, sin\theta_b sin\theta_c \, cos(\varphi_a + \varphi_b + \varphi_c) +$$

$$2\beta\gamma cos\theta_a cos\theta_b sin\theta_c cos\varphi_c, \tag{4.14}$$

We rewrite the Svetlichny function after collecting terms into a sum of four terms,

$$S(\psi_{MS}) = |(\alpha^2 + \beta^2 - \gamma^2)d_1 + 2\alpha\beta d_2 + 2\alpha\gamma d_3 + 2\beta\gamma d_4|, \tag{4.15}$$

where

$$d_1 = cos\theta_a[cos\theta_b(cos\theta_c + cos\theta_{c'}) + cos\theta_{b'}(cos\theta_c - cos\theta_{c'})] +$$
$$cos\theta_{a'}[cos\theta_b(cos\theta_c - cos\theta_{c'}) - cos\theta_{b'}(cos\theta_c + cos\theta_{c'})], \quad (4.16)$$

$$d_2 = sin\theta_a \begin{bmatrix} sin\theta_b cos(\varphi_a + \varphi_b)(cos\theta_c + cos\theta_{c'}) + \\ sin\theta_{b'} cos(\varphi_a + \varphi_{b'})(cos\theta_c - cos\theta_{c'}) \end{bmatrix}$$
$$+ sin\theta_{a'} \begin{bmatrix} sin\theta_b cos(\varphi_{a'} + \varphi_b)(cos\theta_c - cos\theta_{c'}) - \\ sin\theta_{b'} cos(\varphi_{a'} + \varphi_{b'})(cos\theta_c + cos\theta_{c'}) \end{bmatrix}, \quad (4.17)$$

$$d_3 = sin\theta_a \big[sin\theta_b \big(sin\theta_c cos(\varphi_a + \varphi_b + \varphi_c)$$
$$+ sin\theta_{c'} cos(\varphi_a + \varphi_b + \varphi_{c'}) \big)$$
$$+ sin\theta_{b'} \big(sin\theta_c cos(\varphi_a + \varphi_{b'} + \varphi_c) - sin\theta_{c'} cos(\varphi_a + \varphi_{b'} + \varphi_{c'}) \big) \big]$$
$$+ sin\theta_{a'} \big[sin\theta_b \big(sin\theta_c cos(\varphi_{a'} + \varphi_b + \varphi_c)$$
$$- sin\theta_{c'} cos(\varphi_{a'} + \varphi_b + \varphi_{c'}) \big)$$
$$- sin\theta_{b'} \big(sin\theta_c cos(\varphi_{a'} + \varphi_{b'} + \varphi_c)$$
$$+ sin\theta_{c'} cos(\varphi_{a'} + \varphi_{b'} + \varphi_{c'}) \big) \big], \quad (4.18)$$

$$d_4 = cos\theta_a[cos\theta_b(sin\theta_c cos\varphi_c + sin\theta_{c'} cos\varphi_{c'}) +$$
$$cos\theta_{b'}(sin\theta_c cos\varphi_c - sin\theta_{c'} cos\varphi_{c'})] +$$
$$cos\theta_{a'}[cos\theta_b(sin\theta_c cos\varphi_c - sin\theta_{c'} cos\varphi_{c'}) -$$
$$cos\theta_{b'}(sin\theta_c cos\varphi_c + sin\theta_{c'} cos\varphi_{c'})]. \quad (4.19)$$

As before, the maximum value of Svetlichny inequality achieved by MS class states is $4\sqrt{2}$ at $\alpha = \gamma = 1/\sqrt{2}$ and $\beta = 0$ as shewn in figure 4.2 (p. 21). Furthermore, the surface of the plot in figure 4.2 (a) is not centered because of the normalized condition $(\alpha^2 + \beta^2 + \gamma^2 = 1)$. For instance, if $\alpha^2 + \beta^2 > 1$, then $\gamma^2 < 0$. Therefore, the normalized condition prevents any negative value and makes it an empty value. This causes the surface to be located on one side of the graph. The behavior of S_{max} decreases first and then increases smoothly. As β^2 increases, S_{max} decreases until it reaches the bound of 4 as indicated in figure 4.2 (a). Figure 4.2 (b) shows the side view of the 3D

plot when $\beta^2 = 0$ (when we substitute $\beta = 0$ in (4.3), it becomes identical to (4.2)), so it is similar to figure 4.1. Therefore, this confirms that our numerical calculation is correct.

(a)   (b)
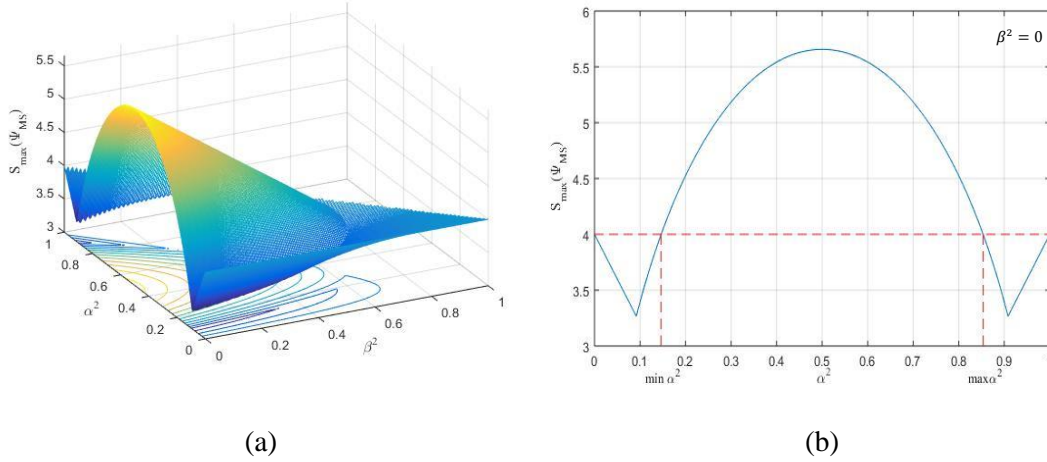
Figure 4.2: (a) The maximal violation of the Svetlichny inequality revealing genuine tripartite non-locality described by (4.15) is plotted versus α^2 and β^2. A contour plot is shown under a wireframe mesh. (b) The side view of (a) shows maxima at $\alpha^2 = 0.5$ by fixing $\beta^2 = 0$.

Figure 4.3 (p. 22) shows 2D slices of the 3D plot by fixing β^2 at constant values. We can clearly see how the shape of S_{max} changes when we vary β^2. Increasing the value of β^2 causes the maximum value to decrease, and the corresponding value of α^2 for which S_{max} is maximized is different for each plot (figures 4.3 (a) and (b)). As a result, all 3-parameter states that exist between $min \, \alpha^2$ and $max \, \alpha^2$ achieve the bound of 4. In addition, the right side of the plot (figures 4.3 (a)) decreases until it vanishes (figure 4.3 (b)). An interesting change occurs at $\beta^2 = 0.6$ and 0.8 as it can be seen in figure 4.3 (c) and (d), and therefore not all 3-parameter states violate the bound of 4 set by local hidden variable theories.
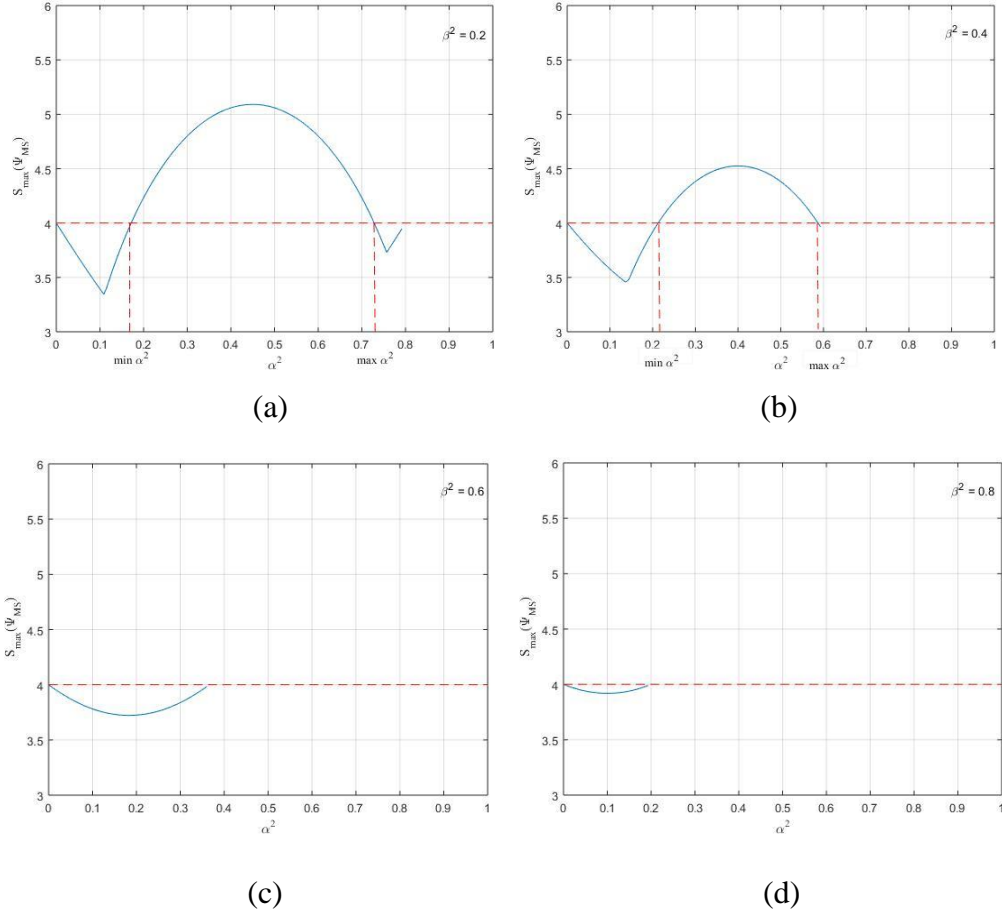
Figure 4.3: Numerically calculated S_{max} as a function of α and γ for the 3-parameter states in (4.15) as β^2 is varied.

4.3   W class states

In this section, we explore W class states:

$$|\psi_W\rangle = \alpha|001\rangle + \beta|010\rangle + \gamma|100\rangle, \qquad \alpha^2 + \beta^2 + \gamma^2 = 1. \qquad (4.20)$$

By defining terms as before, we can express the term $\langle ABC\rangle$ with respect to $|\psi_W\rangle$ as:

$\langle ABC\rangle = -cos\theta_a cos\theta_b cos\theta_c + 2\alpha\beta \cos\theta_a \, sin\theta_b sin\theta_c cos(\varphi_b - \varphi_c) +$

$2\alpha\gamma sin\theta_a cos\theta_b sin\theta_c cos(\varphi_a - \varphi_c) + 2\beta\gamma sin\theta_a sin\theta_b cos\theta_c cos(\varphi_a - \varphi_b). \quad (4.21)$

Similarly, by adding all the eight terms, one can obtain the Svetlichny operator as:

$$S(\psi_W) = |p_1 + 2\alpha\beta p_2 + 2\alpha\gamma p_3 + 2\beta\gamma p_4|, \tag{4.22}$$

where

$$p_1 = -\cos\theta_a[\cos\theta_b(\cos\theta_c + \cos\theta_{c'}) + \cos\theta_{b'}(\cos\theta_c - \cos\theta_{c'})] -$$
$$\cos\theta_{a'}[\cos\theta_b(\cos\theta_c - \cos\theta_{c'}) - \cos\theta_{b'}(\cos\theta_c + \cos\theta_{c'})], \tag{4.23}$$

$$p_2 = \cos\theta_a[\sin\theta_b(\sin\theta_c\cos(\varphi_b - \varphi_c) + \sin\theta_{c'}\cos(\varphi_b - \varphi_{c'}))$$
$$+ \sin\theta_{b'}(\sin\theta_c\cos(\varphi_{b'} - \varphi_c) - \sin\theta_{c'}\cos(\varphi_{b'} - \varphi_{c'}))]$$
$$+ \cos\theta_{a'}[\sin\theta_b(\sin\theta_c\cos(\varphi_b - \varphi_c) - \sin\theta_{c'}\cos(\varphi_b - \varphi_{c'}))$$
$$- \sin\theta_{b'}(\sin\theta_c\cos(\varphi_{b'} - \varphi_c) + \sin\theta_{c'}\cos(\varphi_{b'} - \varphi_{c'}))], \tag{2.24}$$

$$p_3 = \sin\theta_a[\cos\theta_b(\sin\theta_c\cos(\varphi_a - \varphi_c) + \sin\theta_{c'}\cos(\varphi_a - \varphi_{c'}))$$
$$+ \cos\theta_{b'}(\sin\theta_c\cos(\varphi_a - \varphi_c) - \sin\theta_{c'}\cos(\varphi_a - \varphi_{c'}))]$$
$$+ \sin\theta_{a'}[\cos\theta_b(\sin\theta_c\cos(\varphi_{a'} - \varphi_c) - \sin\theta_{c'}\cos(\varphi_{a'} - \varphi_{c'}))$$
$$- \cos\theta_{b'}(\sin\theta_c\cos(\varphi_{a'} - \varphi_c) + \sin\theta_{c'}\cos(\varphi_{a'} - \varphi_{c'}))], \tag{4.25}$$

$$p_4 = \sin\theta_a[\sin\theta_b\cos(\varphi_a - \varphi_b)(\cos\theta_c + \cos\theta_{c'})$$
$$+ \sin\theta_{b'}\cos(\varphi_a - \varphi_{b'})(\cos\theta_c - \cos\theta_{c'})]$$
$$+ \sin\theta_{a'}[\sin\theta_b\cos(\varphi_{a'} - \varphi_b)(\cos\theta_c - \cos\theta_{c'})$$
$$- \sin\theta_{b'}\cos(\varphi_{a'} - \varphi_{b'})(\cos\theta_c + \cos\theta_{c'})]. \tag{4.26}$$

From the above expressions, in figure 4.4 (p. 24), the maximum value (4.354) is obtained for $\alpha = \beta = \gamma = \frac{1}{\sqrt{3}}$. The values of $\alpha, \beta,$ and γ that violate the bound of 4 show that 3-qubit states are non-local. The surface also shifts to one side due to the normalized condition. More interestingly, the shape of the surface is initially constant at 4 and then increases.
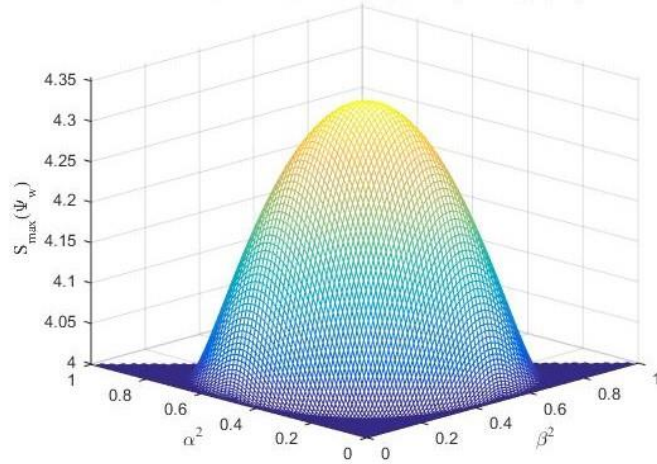
Figure 4.4: $S(\psi_W)_{max}$ is numerically calculated as a function of α and β for the 3-parameter states in (4.22).

Figure 4.5 (p. 25) shows slices of the 3D plot (figure 4.4) by fixing β^2 at a constant value. As we vary β^2, the shape of the $S(\psi_W)_{max}$ surface as a function of α^2 and γ^2 changes. In addition, each plot (figures 4.5 (b - f)) has a different maximum value corresponding to the value of α^2. It can be seen that figure 4.5 (c) shows the side view of figure 4.4 because it gives the same maximum value when $\alpha^2 = \beta^2 = \gamma^2 = 1/3$. Moreover, when β^2 is less or greater than $1/3$, the maximum value decreases. But when $\beta^2 = 0$ (figure 4.5 (a)), W states do not violate the SI ($S \leq 4$) which means the 3-qubit states are not entangled. Therefore, the state $|\psi_W\rangle = \alpha|001\rangle + \gamma|100\rangle$ can be written as a product state of two of the qubits and the remaining qubit as follows:

$$|\psi_W\rangle = \alpha|001\rangle + \gamma|100\rangle,$$
$$|\psi_W\rangle = \alpha|0\rangle_A|0\rangle_B|1\rangle_C + \gamma|1\rangle_A|0\rangle_B|0\rangle_C,$$
$$|\psi_W\rangle = |0\rangle_B(\alpha|0\rangle_A|1\rangle_C + \gamma|1\rangle_A|0\rangle_C),$$

Thus,

$$|\psi_W\rangle = |0\rangle(\alpha|01\rangle + \gamma|10\rangle),$$

where the $\alpha|01\rangle + \gamma|10\rangle$ is the entangled Bell's state with $\alpha = \gamma = 1/\sqrt{2}$.
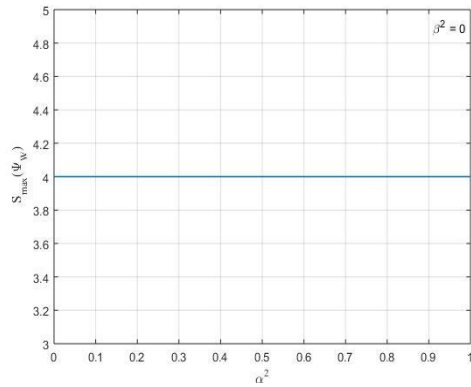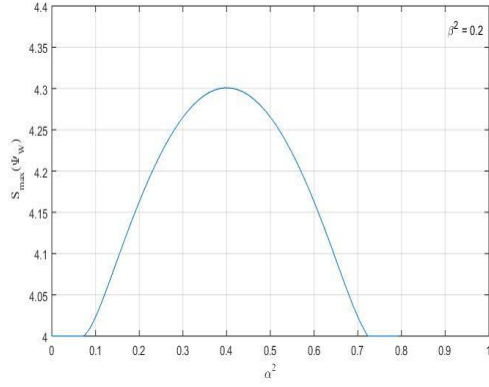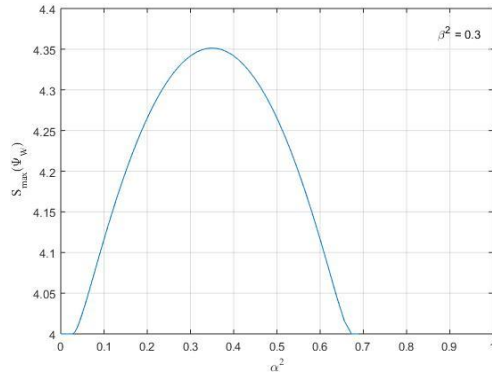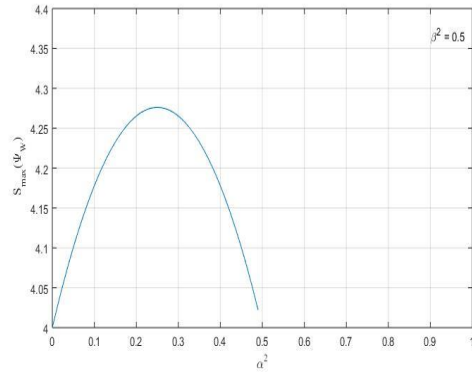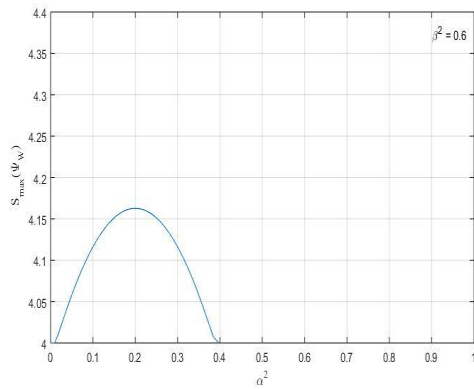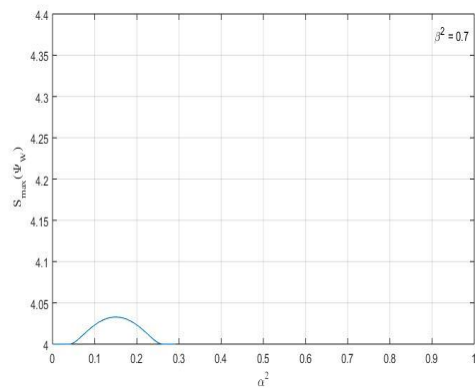
Figure 4.5: The side view of S_{max} numerically calculated as a function of α and β for the 3-parameter states in (4.22) when β^2 is fixed at a constant value.

We can compare our calculation to the results presented in [32]. The formula in this paper is actually derived from Mermin's inequalities (for more information, see [33]) as follows:

$$S = M + M', \qquad (4.27)$$

with

$$M = |\langle ABC' + AB'C + A'BC - A'B'C' \rangle| \leq 2, \qquad (4.28)$$

$$M' = |\langle ABC + AB'C' + A'BC' - A'B'C \rangle| \leq 2. \qquad (4.29)$$

Thus, (4.27) is formally identical to inequality (4.1) as:

$$S = |\langle ABP + AB'P' + A'BP' - A'B'P' \rangle| = M + M'. \qquad (4.30)$$

each term $\langle ABC \rangle$ in (4.30) can be expressed as (4.21). Now adding all the terms in (4.30) and substituting $\varphi_i = 0$, we obtain the expectation of Mermin operator:

$$
\begin{aligned}
\langle M \rangle = \frac{1}{4} \Big[& (-1 - C_{31} - C_{12} - C_{23})\{ cos(\theta_a + \theta_b + \theta_{c'}) + cos(\theta_{a'} + \theta_b + \theta_c) + \\
& cos(\theta_a + \theta_{b'} + \theta_c) - cos(\theta_{a'} + \theta_{b'} + \theta_{c'}) \} + \\
& (-1 + C_{31} + C_{12} - C_{23})\{ cos(\theta_a + \theta_b - \theta_{c'}) + cos(\theta_{a'} + \theta_b - \theta_c) + \\
& cos(\theta_a + \theta_{b'} - \theta_c) - cos(\theta_{a'} + \theta_{b'} - \theta_{c'}) \} + \\
& (-1 - C_{31} + C_{12} + C_{23})\{ cos(\theta_a - \theta_b + \theta_{c'}) + cos(\theta_{a'} - \theta_b + \theta_c) + \\
& cos(\theta_a - \theta_{b'} + \theta_c) - cos(\theta_{a'} - \theta_{b'} + \theta_{c'}) \} + \\
& (-1 + C_{31} - C_{12} + C_{23})\{ cos(\theta_a - \theta_b - \theta_{c'}) + cos(\theta_{a'} - \theta_b - \theta_c) + \\
& cos(\theta_a - \theta_{b'} - \theta_c) - cos(\theta_{a'} - \theta_{b'} - \theta_{c'}) \} \Big],
\end{aligned} \qquad (4.31)
$$

where $C_{12} = 2\alpha\beta, C_{23} = 2\beta\gamma$, and $C_{31} = 2\gamma\alpha$.

Similarly, we can find the expression for $\langle M' \rangle$. θ_i's can be suitably expressed by defining $\bar{\theta}_g = \frac{\theta_g + \theta_{g'}}{2}, \tilde{\theta}_g = \frac{\theta_{g'} - \theta_g}{2}, \ g \in \{a, b, c\}$. Allowing $\Sigma = (\tilde{\theta}_a + \tilde{\theta}_b + \tilde{\theta}_c)$ and $\Sigma_g = \Sigma - 2\tilde{\theta}_g$, we have:

$$S(\psi_W) = \frac{1}{2} \left[(-1 - C_{31} - C_{12} - C_{23}) \sin(\bar{\theta}_a + \bar{\theta}_b + \bar{\theta}_c) \left\{ G - 2\sin(\tilde{\theta}_a - \tilde{\theta}_b - \tilde{\theta}_c) \right\} \right.$$

$$+ (-1 + C_{31} + C_{12} - C_{23}) \sin(\bar{\theta}_a + \bar{\theta}_b - \bar{\theta}_c) \left\{ G - 2\sin(\tilde{\theta}_a - \tilde{\theta}_b + \tilde{\theta}_c) \right\}$$

$$+ (-1 - C_{31} + C_{12} + C_{23}) \sin(\bar{\theta}_a - \bar{\theta}_b + \bar{\theta}_c) \left\{ G - 2\sin(\tilde{\theta}_a + \tilde{\theta}_b - \tilde{\theta}_c) \right\}$$

$$+ \left. (-1 + C_{31} - C_{12} + C_{23}) \sin(\tilde{\theta}_a - \tilde{\theta}_b - \tilde{\theta}_c) \left\{ G - 2\sin(\tilde{\theta}_a + \tilde{\theta}_b + \tilde{\theta}_c) \right\} \right], \quad (4.32)$$

with

$$G = \left\{ \sin(\tilde{\theta}_a + \tilde{\theta}_b + \tilde{\theta}_c) + \sin(\tilde{\theta}_a + \tilde{\theta}_b - \tilde{\theta}_c) + \sin(\tilde{\theta}_a - \tilde{\theta}_b + \tilde{\theta}_c) \right.$$

$$\left. + \sin(\tilde{\theta}_a - \tilde{\theta}_b - \tilde{\theta}_c) \right\}. \quad (4.33)$$

We rearrange (4.32) by substituting $\bar{\theta}_a = \bar{\theta}_b = \bar{\theta}_c = \frac{\pi}{2}$ as:

$$S(\psi_w) = (p_1 + p_2 C_{31} + p_3 C_{12} + p_4 C_{23}), \quad (4.34)$$

where

$$p_1 = -\sin\Sigma + \sin\Sigma_a + \sin\Sigma_b + \sin\Sigma_c, \quad (4.35)$$

$$p_2 = \sin\Sigma + \sin\Sigma_a - \sin\Sigma_b + \sin\Sigma_c, \quad (4.36)$$

$$p_3 = \sin\Sigma - \sin\Sigma_a + \sin\Sigma_b + \sin\Sigma_c, \quad (4.37)$$

$$p_4 = \sin\Sigma + \sin\Sigma_a + \sin\Sigma_b - \sin\Sigma_c. \quad (4.38)$$

Therefore, by using (4.34), we obtain a graph that is similar to figure 4.4. Thus, our calculation verifies the formula in [32].

Chapter 5

Four Qubit Entanglement

In this chapter, we show that the 3-qubit analysis in the previous chapter can be generalized to the case of 4-qubit states to obtain a relationship between 4-qubit entanglement and non-locality.

In the future, this approach could then be expanded to the N-qubit case, where N is large, for which numerical studies are very challenging [31]. The set-up of 4-qubit states is similar to the two and three qubit cases described in the previous chapters. Each qubit is subjected to local projection measurements in one of two randomly chosen bases or directions. The value of a correlation function such as the 4-qubit Bell-type operator M_4 can be calculated as:

$$M_4 = |\langle ABQ + AB'Q' + A'BQ' - A'B'Q' \rangle|, \tag{5.1}$$

with $Q = C(D - D') - C'(D + D')$ and $Q' = C'(D' - D) - C(D + D')$. D and D' are the operators corresponding to local measurements made by Diana on qubit 4 in one of the two directions [31]. The function M_4 in (5.1) is always bounded by a value of 8 ($M_4 \leq 8$) when non-local correlations are allowed between at most three of the four qubits. However, based on our analysis of 3-qubit states, we expect to obtain the violaton of inequality $M_4 \leq 8$ using 4-qubit generalized GHZ states and MS states. Violation of this inequality is a sufficient condition for identifying genuine 4-qubit non-locality. However, our expectation for 4-qubit W states is that we may not obtain the violation of inequality $M_4 \leq 8$ because we notice that in the 3-qubit case, the difference between the maximum value of W states ($S(\psi_W)_{max} = 4.35$) and the bound of 4 set by local hidden variable is only 0.35. Another possible reason is that the degree of

quantum non-locality depends not only on the given entangled state but also on the Bell operator.

5.1   Generalized GHZ States (GGHZ)

Given the 4-qubit GGHZ states:

$$|\psi_G\rangle = \alpha|0000\rangle + \beta|1111\rangle, \qquad \alpha^2 + \beta^2 = 1. \tag{5.2}$$

each term in the 4-qubit Bell parameter M_4 (5.1) can be expressed as:

$$\langle ABCD\rangle = cos\theta_a cos\theta_b cos\theta_c cos\theta_d + 2\alpha\beta\ sin\theta_a sin\theta_b sin\theta_c sin\theta_d cos\varphi_{abcd}, \tag{5.3}$$

Where

$$\varphi_{abcd} = \varphi_a + \varphi_b + \varphi_c + \varphi_d.$$

Thus, we can collect terms so that M_4 can be written as a sum of two terms,

$$M_4 = |c_1 + 2\alpha\beta c_2|, \tag{5.4}$$

where

$$c_1 = cos\theta_a cos\theta_b f_Q + cos\theta_a cos\theta_{b\prime} f_{Q\prime} + cos\theta_{a\prime} cos\theta_b f_{Q\prime} - cos\theta_{a\prime} cos\theta_{b\prime} f_Q, \tag{5.5}$$

$$c_2 = sin\theta_a sin\theta_b h_{ab} + sin\theta_a sin\theta_{b\prime} h_{ab\prime} + sin\theta_{a\prime} sin\theta_b h_{a\prime b} - sin\theta_{a\prime} sin\theta_{b\prime} h_{a\prime b\prime}, \tag{5.6}$$

with

$$f_Q = cos\theta_c(cos\theta_d - cos\theta_{d\prime}) - cos\theta_{c\prime}(cos\theta_d + cos\theta_{d\prime}), \tag{5.7}$$

$$f_{Q\prime} = cos\theta_{c\prime}(cos\theta_{d\prime} - cos\theta_d) - cos\theta_c(cos\theta_d + cos\theta_{d\prime}), \tag{5.8}$$

$$h_{ab} = sin\theta_c(sin\theta_d\ cos\varphi_{abcd} - sin\theta_{d\prime} cos\varphi_{abcd\prime}) -$$
$$sin\theta_{c\prime}(sin\theta_d cos\varphi_{abc\prime d} + sin\theta_{d\prime} cos\varphi_{abc\prime d\prime}), \tag{5.9}$$

$$h_{ab\prime} = sin\theta_{c\prime}(sin\theta_{d\prime} cos\varphi_{ab\prime c\prime d\prime} - sin\theta_d cos\varphi_{ab\prime c\prime d}) -$$
$$sin\theta_c(sin\theta_d cos\varphi_{ab\prime cd} + sin\theta_{d\prime} cos\varphi_{ab\prime cd\prime}), \tag{5.10}$$

$$h_{a\prime b} = sin\theta_{c\prime}(sin\theta_{d\prime} cos\varphi_{a\prime bc\prime d\prime} - sin\theta_d cos\varphi_{a\prime bc\prime d}) -$$
$$sin\theta_c(sin\theta_d cos\varphi_{a\prime bcd} + sin\theta_{d\prime} cos\varphi_{a\prime bcd\prime}), \tag{5.11}$$

$$h_{a\prime b\prime} = sin\theta_c(sin\theta_d cos\varphi_{a\prime b\prime cd} - sin\theta_{d\prime} cos\varphi_{a\prime b\prime cd\prime}) -$$
$$sin\theta_{c\prime}(sin\theta_d cos\varphi_{a\prime b\prime c\prime d} + sin\theta_{d\prime} cos\varphi_{a\prime b\prime c\prime d\prime}). \tag{5.12}$$

As a result, we have obtained the following plot (figure 5.1) for the maximum value of M_4 for the 4-qubit GGHZ states using Matlab. In figure 5.1, there are several interesting points to be noted. The general behavior of M_{max} is similar to S_{max} for the 3-qubit case which is: Firstly, as α^2 increases, M_{max} does not vary smoothly. Secondly, M_{max} is initially constant whereas S_{max} decreases first and then increases. Furthermore, there is a sharp change in the behavior of M_{max} like S_{max}, and the change occurs at a different value of α^2.

This corresponds to a change in the optimal measurements of the 4-qubit states from measurements along the z-axis to measurements in the xy-plane $\theta = \pi/2$, as in the 3-qubit case [31]. There exist 4-qubit GGHZ states with genuine multiqubit entanglement that nevertheless do not violate the Bell-type inequality in (5.1). A final interesting observation is that the critical point of the values of α^2 that is labeled by $min\ \alpha^2$ and $max\ \alpha^2$ beyond which there is a violation is identical for the 3-qubit and 4-qubit case. The maximum $8\sqrt{2}$ occurs at $\alpha = \beta = 1/\sqrt{2}$.
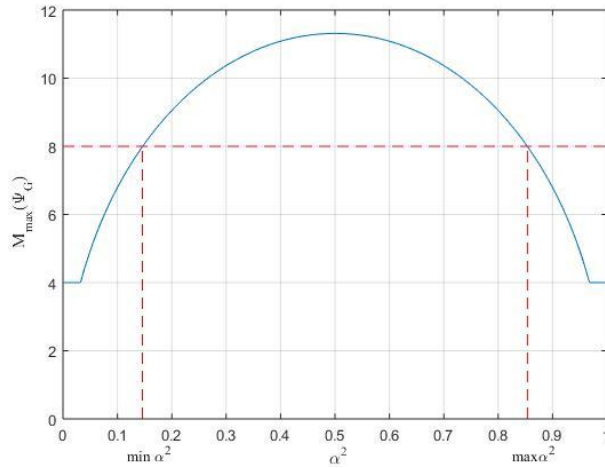
Figure 5.1. Numerical calculations of M_{max} from the expression derived in (5.4) (solid line). The horizontal dashed line shows the bound of 8 set by models in which nonlocal correlations can exist between at most three qubits. In contrast, the vertical dashed lines show important values of α^2 that violate the bound of 8.

5.2   Maximal Slice (MS) States

Consider the 4-qubit MS states:

$$|\psi_{MS}\rangle = \alpha|0000\rangle + \beta|1110\rangle + \gamma|1111\rangle, \quad \alpha^2 + \beta^2 + \gamma^2 = 1. \quad (5.13)$$

We can express each term in (5.1) as:

$\langle ABCD \rangle =$

$(\alpha^2 - \beta^2 + \gamma^2)\cos\theta_a\cos\theta_b\cos\theta_c\cos\theta_d + 2\alpha\beta\cos\theta_d\sin\theta_a\sin\theta_b\sin\theta_c\cos\varphi_{abc} +$

$2\alpha\gamma\sin\theta_a\sin\theta_b\sin\theta_c\sin\theta_d\cos\varphi_{abcd} - 2\beta\gamma\cos\theta_a\cos\theta_b\cos\theta_c\sin\theta_d\cos\varphi_d, \quad (5.14)$

with

$$\varphi_{abc} = \varphi_a + \varphi_b + \varphi_c,$$

$$\varphi_{abcd} = \varphi_a + \varphi_b + \varphi_c + \varphi_d.$$

By collecting terms, we rearrange the 4-qubit Bell parameter M_4 into a sum of four terms,

$$M_4(MS) = |(\alpha^2 - \beta^2 + \gamma^2)r_1 + 2\alpha\beta r_2 + 2\alpha\gamma r_3 - 2\beta\gamma r_4|, \quad (5.15)$$

where

$r_1 = c_1$ and $r_3 = c_2$ (c_1 and c_2 are introduced in the previous section),

and

$$r_2 = \sin\theta_a\sin\theta_b f_{ab} + \sin\theta_a\sin\theta_{b'}f_{ab'} + \sin\theta_{a'}\sin\theta_b f_{a'b} - \sin\theta_{a'}\sin\theta_{b'}f_{a'b'},$$

$$(5.16)$$

with

$$f_{ab} = \sin\theta_c\cos\varphi_{abc}(\cos\theta_d - \cos\theta_{d'}) - \sin\theta_{c'}\cos\varphi_{abc'}(\cos\theta_d + \cos\theta_{d'}), \quad (5.17)$$

$$f_{ab'} = \sin\theta_{c'}\cos\varphi_{ab'c'}(\cos\theta_{d'} - \cos\theta_d) - \sin\theta_c\cos\varphi_{ab'c}(\cos\theta_d + \cos\theta_{d'}),$$

$$(5.18)$$

$$f_{a'b} = \sin\theta_{c'}\cos\varphi_{a'bc'}(\cos\theta_{d'} - \cos\theta_d) - \sin\theta_c\cos\varphi_{a'bc}(\cos\theta_d + \cos\theta_{d'}),$$

$$(5.19)$$

$$f_{a'b'} = \sin\theta_c\cos\varphi_{a'b'c}(\cos\theta_d - \cos\theta_{d'}) - \sin\theta_{c'}\cos\varphi_{a'b'c'}(\cos\theta_d + \cos\theta_{d'}).$$

$$(5.20)$$

$$r_4 = cos\theta_a cos\theta_b f_N + cos\theta_a cos\theta_{b'} f_{N'} + cos\theta_{a'} cos\theta_b f_{N'} - cos\theta_{a'} cos\theta_{b'} f_N,$$

$$(5.21)$$

with

$$f_N = cos\theta_c(sin\theta_d cos\varphi_d - sin\theta_{d'} cos\varphi_{d'})$$
$$-cos\theta_{c'}(sin\theta_d cos\varphi_d + sin\theta_{d'} cos\varphi_{d'}), \qquad (5.22)$$
$$f_{N'} = cos\theta_{c'}(sin\theta_{d'} cos\varphi_{d'} - sin\theta_d cos\varphi_d)$$
$$-cos\theta_c(sin\theta_d cos\varphi_d + sin\theta_{d'} cos\varphi_{d'}). \qquad (5.23)$$

The maximum of (5.15) is shown in figure 5.2. The general behavior of M_{max} is similar to S_{max} for the 3-qubit case (figure 4.2), and the explanation is the same. The maximal violation of the Bell-inequality reaches its maximum 8 ($8\sqrt{2}$) for the 4-qubit MS states at $\alpha = \gamma = 1/\sqrt{2}$, and $\beta = 0$. Thus, these states are genuinely multiqubit entangled.
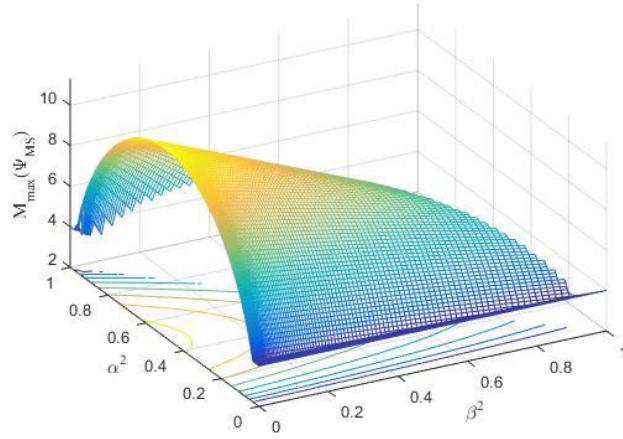
Figure 5.2: The maximal violation of 4-qubit Bell parameter M_4 revealing genuine tripartite non-locality described by (5.15), and is plotted versus α^2 and β^2. γ^2 is a function of α^2 and β^2.

Figure 5.3 (p. 33) shows slices of the 3D plot (figure 5.2). These side views show more clearly how the surface of M_{max} changes. The measurement varies smoothly with the value of quantum violation. Figure 5.3 (a) is identical to figure 5.1 when β^2

is fixed at a constant value equal to zero. Moreover, as the 4-qubit entanglement is decreased further (figure 5.3 (b) and (c)), a larger proportion of states lie below the bound of 8. In other words, the critical points of α^2, labeled by $min\ \alpha^2$ and $max\ \alpha^2$, beyond which there is a violation are shrinking. There is no violation in figure 5.3 (d).
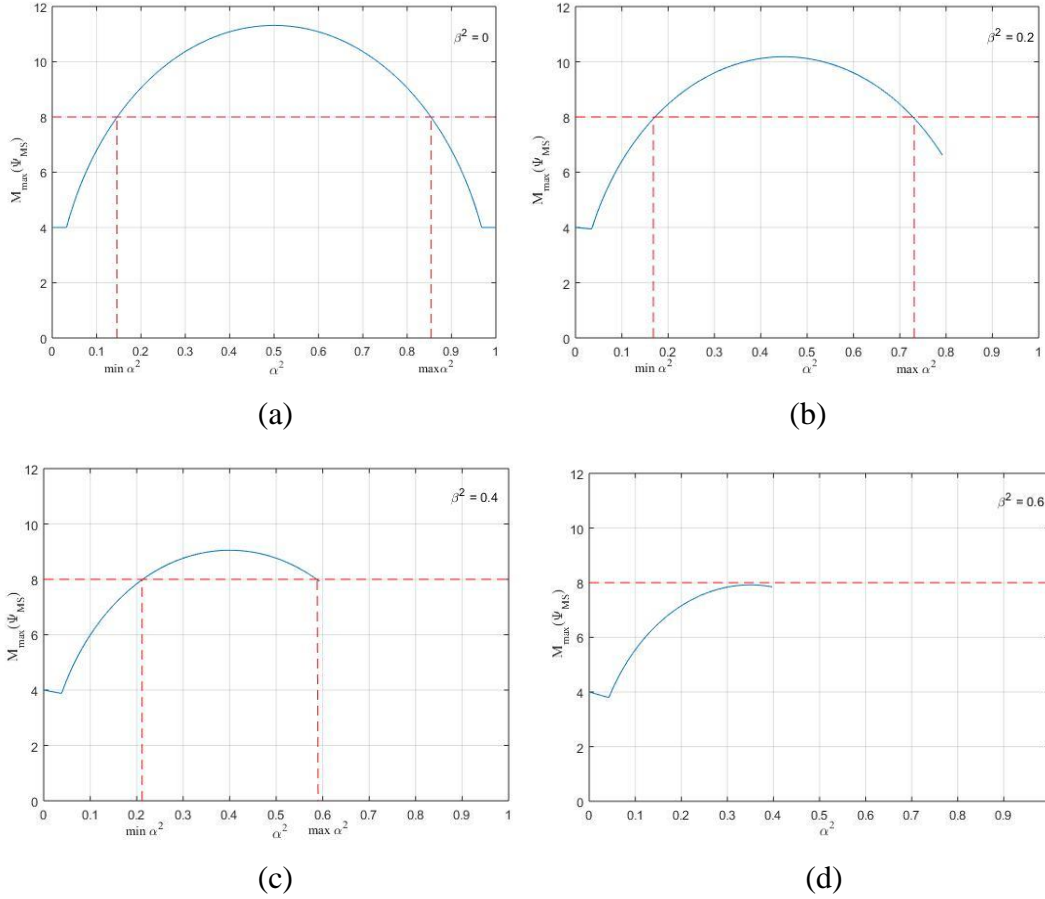
Figure 5.3: Numerically calculated M_{max} as a function of α and γ for the 4-parameter states in (5.15) as β^2 is varied.

5.3   W Class States

The 4-qubit W states takes the form:

$$|\psi_W\rangle = \alpha|0001\rangle + \beta|0010\rangle + \gamma|0100\rangle + \delta|1000\rangle, \tag{5.24}$$

where the complex parameters α, β, γ and δ satisfy the normalization condition:

$$\alpha^2 + \beta^2 + \gamma^2 + \delta^2 = 1.$$

each term in the 4-qubit Bell parameter M_4 (5.1) can be expressed as:

$$\langle ABCD \rangle = -cos\theta_a cos\theta_b cos\theta_c cos\theta_d +$$
$$2\alpha\beta cos\theta_a cos\theta_b sin\theta_c sin\theta_d cos(\varphi_c - \varphi_d) +$$
$$2\alpha\gamma cos\theta_a sin\theta_b cos\theta_c sin\theta_d cos(\varphi_b - \varphi_d) +$$
$$2\gamma\beta cos\theta_a sin\theta_b sin\theta_c cos\theta_d cos(\varphi_b - \varphi_c) +$$
$$2\alpha\delta sin\theta_a cos\theta_b cos\theta_c sin\theta_d cos(\varphi_a - \varphi_d) +$$
$$2\beta\delta sin\theta_a cos\theta_b sin\theta_c cos\theta_d cos(\varphi_a - \varphi_c) +$$
$$2\alpha\delta sin\theta_a sin\theta_b cos\theta_c cos\theta_d cos(\varphi_a - \varphi_b). \qquad (5.25)$$

Then by collecting terms, we rearrange the 4-qubit Bell parameter M_4 function into a sum of seven terms as:

$$M_4(W) = |q_1 + 2\alpha\beta q_2 + 2\alpha\gamma q_3 + 2\gamma\beta q_4 + 2\alpha\delta q_5 + 2\beta\delta q_6 + 2\alpha\delta q_7|, \quad (5.26)$$

where

$q_1 = -c_1$ (c_1 is introduced in the previous section),

$$q_2 = cos\theta_a cos\theta_b f_R + cos\theta_a cos\theta_{b'} f_{R'} + cos\theta_{a'} cos\theta_b f_{R'} - cos\theta_{a'} cos\theta_{b'} f_R, (5.27)$$

$$f_R = sin\theta_c[sin\theta_d \, cos(\varphi_c - \varphi_d) - sin\theta_{d'} \, cos(\varphi_c - \varphi_{d'})]$$
$$-sin\theta_{c'}[sin\theta_d cos(\varphi_{c'} - \varphi_d) + sin\theta_{d'} cos(\varphi_{c'} - \varphi_{d'})], \qquad (5.28)$$

$$f_{R'} = sin\theta_{c'}[sin\theta_{d'} cos(\varphi_{c'} - \varphi_{d'}) - sin\theta_d cos(\varphi_{c'} - \varphi_d)]$$
$$-sin\theta_c[sin\theta_d cos(\varphi_c - \varphi_d) + sin\theta_{d'} cos(\varphi_c - \varphi_{d'})]. \qquad (5.29)$$

$$q_3 = cos\theta_a sin\theta_b k_{ab} + cos\theta_a sin\theta_{b'} k_{ab'} + cos\theta_{a'} sin\theta_b k_{a'b} - cos\theta_{a'} sin\theta_{b'} k_{a'b'},$$
$$(5.30)$$

here

$$k_{ab} = cos\theta_c \big(sin\theta_d cos(\varphi_b - \varphi_d) - sin\theta_{d'} cos(\varphi_b - \varphi_{d'}) \big)$$
$$-cos\theta_{c'} \big(sin\theta_d cos(\varphi_b - \varphi_d) + sin\theta_{d'} cos(\varphi_b - \varphi_{d'}) \big), \qquad (5.31)$$

$$k_{ab'} = cos\theta_{c'} \big(sin\theta_{d'} cos(\varphi_{b'} - \varphi_{d'}) - sin\theta_d cos(\varphi_{b'} - \varphi_d) \big)$$
$$-cos\theta_c \big(sin\theta_d cos(\varphi_{b'} - \varphi_d) + sin\theta_{d'} cos(\varphi_{b'} - \varphi_{d'}) \big), \qquad (5.32)$$

$$k_{a'b} = cos\theta_{c'}\big(sin\theta_{d'}cos(\varphi_b - \varphi_{d'}) - sin\theta_d cos(\varphi_b - \varphi_d)\big)$$
$$-cos\theta_c\big(sin\theta_d cos(\varphi_b - \varphi_d) + sin\theta_{d'}cos(\varphi_b - \varphi_{d'})\big), \qquad (5.33)$$

$$k_{a'b'} = cos\theta_c\big(sin\theta_d cos(\varphi_{b'} - \varphi_d) - sin\theta_{d'}cos(\varphi_{b'} - \varphi_{d'})\big)$$
$$-cos\theta_{c'}\big(sin\theta_d cos(\varphi_{b'} - \varphi_d) + sin\theta_{d'}cos(\varphi_{b'} - \varphi_{d'})\big). \qquad (5.34)$$

$$q_4 = cos\theta_a sin\theta_b v_{ab} + cos\theta_a sin\theta_{b'} v_{ab'} + cos\theta_{a'}sin\theta_b v_{a'b} - cos\theta_{a'}sin\theta_{b'} v_{a'b'},$$
$$(5.35)$$

with

$$v_{ab} = sin\theta_c cos(\varphi_b - \varphi_c)(cos\theta_d - cos\theta_{d'})$$
$$-sin\theta_{c'}cos(\varphi_b - \varphi_{c'})(cos\theta_d + cos\theta_{d'}), \qquad (5.36)$$

$$v_{ab'} = sin\theta_{c'}cos(\varphi_{b'} - \varphi_{c'})(cos\theta_{d'} - cos\theta_d)$$
$$-sin\theta_c cos(\varphi_{b'} - \varphi_c)(cos\theta_d + cos\theta_{d'}), \qquad (5.37)$$

$$v_{a'b} = sin\theta_{c'}cos(\varphi_b - \varphi_{c'})(cos\theta_{d'} - cos\theta_d)$$
$$-sin\theta_c cos(\varphi_b - \varphi_c)(cos\theta_d + cos\theta_{d'}), \qquad (5.38)$$

$$v_{a'b'} = sin\theta_c cos(\varphi_{b'} - \varphi_c)(cos\theta_d - cos\theta_{d'})$$
$$-sin\theta_{c'}cos(\varphi_{b'} - \varphi_{c'})(cos\theta_d + cos\theta_{d'}). \qquad (5.39)$$

$$q_5 = sin\theta_a cos\theta_b g_{ab} + sin\theta_a cos\theta_{b'} g_{ab'} + sin\theta_{a'}cos\theta_b g_{a'b} - sin\theta_{a'}cos\theta_{b'} g_{a'b'},$$
$$(5.40)$$

and

$$g_{ab} = cos\theta_c\big(sin\theta_d cos(\varphi_a - \varphi_d) - sin\theta_{d'}cos(\varphi_a - \varphi_{d'})\big)$$
$$-cos\theta_{c'}\big(sin\theta_d cos(\varphi_a - \varphi_d) + sin\theta_{d'}cos(\varphi_a - \varphi_{d'})\big), \quad (5.41)$$

$$g_{ab'} = cos\theta_{c'}\big(sin\theta_{d'}cos(\varphi_a - \varphi_{d'}) - sin\theta_d cos(\varphi_a - \varphi_d)\big)$$
$$-cos\theta_c\big(sin\theta_d cos(\varphi_a - \varphi_d) + sin\theta_{d'}cos(\varphi_a - \varphi_{d'})\big), \quad (5.42)$$

$$g_{a'b} = cos\theta_{c'}\big(sin\theta_{d'}cos(\varphi_{a'} - \varphi_{d'}) - sin\theta_d cos(\varphi_{a'} - \varphi_d)\big)$$
$$-cos\theta_c\big(sin\theta_d cos(\varphi_{a'} - \varphi_d) + sin\theta_{d'}cos(\varphi_{a'} - \varphi_{d'})\big), \quad (5.43)$$

$$g_{a'b'} = cos\theta_c\big(sin\theta_d cos(\varphi_{a'} - \varphi_d) - sin\theta_{d'}cos(\varphi_{a'} - \varphi_{d'})\big)$$
$$-cos\theta_{c'}\big(sin\theta_d cos(\varphi_{a'} - \varphi_d) + sin\theta_{d'}cos(\varphi_{a'} - \varphi_{d'})\big).(5.44)$$

$$q_6 = sin\theta_a cos\theta_b p_{ab} + sin\theta_a cos\theta_{b'} p_{ab'} + sin\theta_{a'} cos\theta_b p_{a'b} - sin\theta_{a'} cos\theta_{b'} p_{a'b'},$$

$$(5.45)$$

with

$$p_{ab} = sin\theta_c cos(\varphi_a - \varphi_c)(cos\theta_d - cos\theta_{d'})$$
$$-sin\theta_{c'} cos(\varphi_a - \varphi_{c'})(cos\theta_d + cos\theta_{d'}), \qquad (5.46)$$

$$p_{ab'} = sin\theta_{c'} cos(\varphi_a - \varphi_{c'})(cos\theta_{d'} - cos\theta_d)$$
$$-sin\theta_c cos(\varphi_a - \varphi_c)(cos\theta_d + cos\theta_{d'}), \qquad (5.47)$$

$$p_{a'b} = sin\theta_{c'} cos(\varphi_{a'} - \varphi_{c'})(cos\theta_{d'} - cos\theta_d)$$
$$-sin\theta_c cos(\varphi_{a'} - \varphi_c)(cos\theta_d + cos\theta_{d'}), \qquad (5.48)$$

$$p_{a'b'} = sin\theta_c cos(\varphi_{a'} - \varphi_c)(cos\theta_d - cos\theta_{d'})$$
$$-sin\theta_{c'} cos(\varphi_{a'} - \varphi_{c'})(cos\theta_d + cos\theta_{d'}). \qquad (5.49)$$

$$q_7 = sin\theta_a sin\theta_b cos(\varphi_a - \varphi_b)f_U + sin\theta_a sin\theta_{b'} cos(\varphi_a - \varphi_{b'})f_{U'} +$$
$$sin\theta_{a'} sin\theta_b cos(\varphi_{a'} - \varphi_b)f_{U'} - sin\theta_{a'} sin\theta_{b'} cos(\varphi_{a'} - \varphi_{b'})f_U, \qquad (5.50)$$

with

$$f_U = cos\theta_c(cos\theta_d - cos\theta_{d'}) - cos\theta_{c'}(cos\theta_d + cos\theta_{d'}), \qquad (5.51)$$
$$f_{U'} = cos\theta_{c'}(cos\theta_{d'} - cos\theta_d) - cos\theta_c(cos\theta_d + cos\theta_{d'}). \qquad (5.52)$$

Since here we calculate the maximum value, and our function in (5.26) has 4 variables, we cannot plot it in 4D. As a result, we fixed one variable and vary the other two. δ^2 is given from the normalization condition which is:

$$\delta^2 = 1 - \alpha^2 - \beta^2 - \gamma^2.$$

Numerical calculations show when we fixed $\alpha^2, \beta^2,$ or γ^2 at a constant value such as 0, 0.2, 0.4, and 0.6, we have similar results. Thus, we only show one result for which α^2 is fixed as shown in figure 5.4 (p. 37, 38). Figures 5.4 (a - d) do not reveal quantum non-locality since a numerical calculation gives $M_4 \leq 8$. Moreover, figure 5.4 (a) shows that the 4-qubit states are separable which is illustrated as follows:

$$|\psi_W\rangle = \alpha|0001\rangle + \beta|0010\rangle + \gamma|0100\rangle + \delta|1000\rangle,$$
$$|\psi_W\rangle = \alpha|0\rangle_A|0\rangle_B|0\rangle_C|1\rangle_D + \beta|0\rangle_A|0\rangle_B|1\rangle_C|0\rangle_D$$
$$+\gamma|0\rangle_A|1\rangle_B|0\rangle_C|0\rangle_D + \delta|1\rangle_A|0\rangle_B|0\rangle_C|0\rangle_D,$$

Since $\alpha^2 = 0$, we have:

$$|\psi_W\rangle = \beta|0\rangle_A|0\rangle_B|1\rangle_C|0\rangle_D + \gamma|0\rangle_A|1\rangle_B|0\rangle_C|0\rangle_D + \delta|1\rangle_A|0\rangle_B|0\rangle_C|0\rangle_D,$$

$$|\psi_W\rangle = |0\rangle_D(|0\rangle_A|0\rangle_B|1\rangle_C + \gamma|0\rangle_A|1\rangle_B|0\rangle_C + \delta|1\rangle_A|0\rangle_B|0\rangle_C).$$

Similarly, the same explanation can be applied when $\beta^2 = 0$ or $\gamma^2 = 0$.

This illustrates that $|\psi_W\rangle$ cannot exceed the bound of 8. In addition, when we increase the value of α^2, the surface of $M_{max}(\psi_W)$ shrinks and its maximum value increases (figure 5.4 (b)), but still there is no violation. Figures 5.4 (c - d) show that the maximum value decreases and the shape of $M_{max}(\psi_W)$ becomes smaller. Hence, all four qubits in W states do not show non-locality as measured by the Svetlichny's inequality.
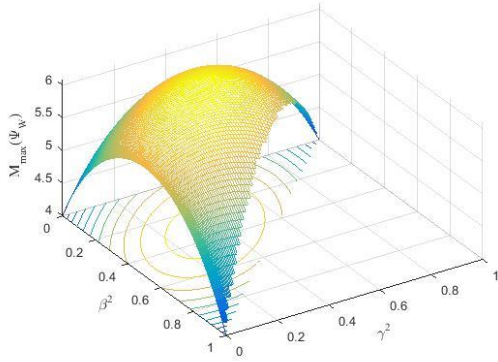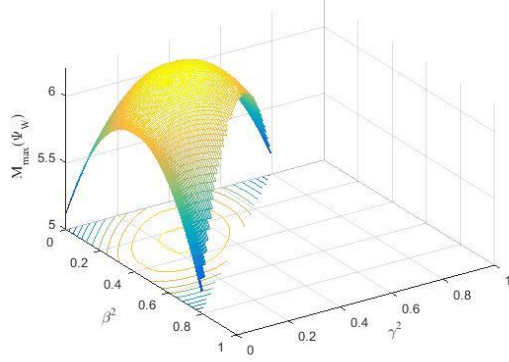
(a) $\alpha^2 = 0$ (b) $\alpha^2 = 0.2$
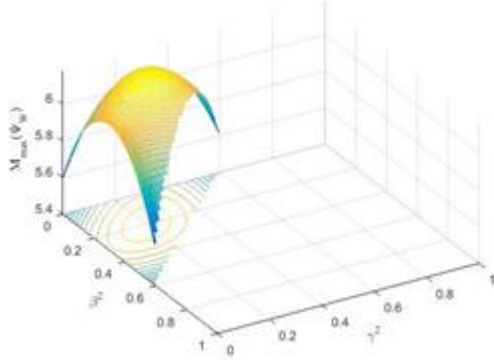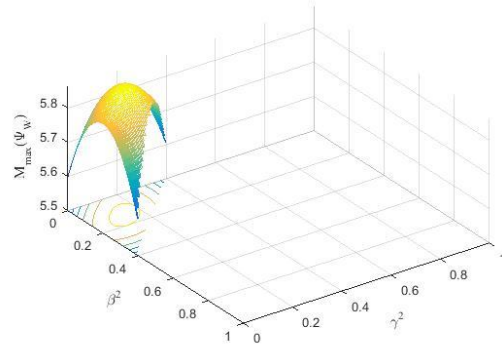
(c) $\alpha^2 = 0.4$ (d) $\alpha^2 = 0.6$

Figure 5.4: $M_{max}(\psi_W)$ is numerically calculated as a function of γ and β for the 5-parameter states in (5.26) as α^2 is varied.

Consequently, the result we have obtained agreed with our expectation. Non violation of 4-qubit W states does not show that quantum mechanics is local realistic, but it is not useful to study the relationship between non-locality and entanglement using 4-qubit Bell parameter $M_4 \leq 8$. Four qubit W states, however, do violate two types of 4-qubit inequalities that were studied in [34] and [35] respectively.

Chunfeng and Jing-Ling numerically calculated the maximum value of the 4-qubit ZB inequality ($\text{ß}_{4qubits} \leq 4$) to be 5.14529 which is greater than 4 [34]. The other inequality that is violated by the 4-qubit W states is a Bell-type operator $\mathcal{B}_{LHV} \leq 2$. Dong, Fengli, and Ting obtained the maximum violation of Bell-type operator $\mathcal{B}_{LHV} \leq 2$ which is 2.5 [35]. The maximum violation of each inequality ($\text{ß}_{4qubits} \leq 4$ or $\mathcal{B}_{LHV} \leq 2$) accrues at $\alpha = \beta = \gamma = \delta = 1/2$. As a result, the inequalities are maximally violated by the 4-qubit W states although they do not violate 4-qubit Bell inequality $M_4 \leq 8$.

Chapter 6
Conclusion

We have seen how the inductive reasoning used by Einstein, Podolsky and Rosen yields the conclusion that the principle of locality, the principle of reality, and the completeness of quantum mechanical description are three postulates incompatible with each other. Indeed, by assuming these three hypotheses, a paradox arises, which led EPR to conclude that quantum theory is somehow incomplete [6]. However, the interpretation of Einstein was opposed by many, including the great quantum physicist, Niels Bohr [19]. Subsequently, John Bell formulated an experiment (known as Bell's inequality) that could be used to test EPR's assumptions [8, 9]. He found that quantum mechanics predicts a violation of his inequality, and therefore it cannot be completed by local hidden variable theories.

In recent years, the analysis of non-locality in pure 2-qubit systems has been well studied [36], and it is well known that all entangled pure states of two qubits can violate Bell inequalities [37]. This thesis is a part of ongoing efforts to explore how far this important 2-qubit relationship between the interesting phenomena of entanglement and non-locality can be extended to the multiqubit case. Here, we have explored the violation of multiqubit Bell inequalities by entangled states. Specifically, we have studied how multiqubit non-locality behaves in certain interesting families of 3 and 4-qubit pure states, namely the GHZ, MS, and W states.

First, we have numerically computed the maximum violation of the Bell-type inequalities developed by Svetlichny that tests for non-local correlations between three qubits [13]. The outcomes of the numerical calculations showed that there is a complex

relationship between entanglement and non-locality in 3-qubit states. Second, by following the same steps as in the 3-qubit case, we have extended our analysis to 4-qubit states that have not been studied before. We calculated the maximum value of a 4-qubit Bell-type operator M_4, that is a generalization of the 3-qubit Svetlichny operator. Thus, we found that 4-qubit GGHZ states and MS states are similar to the 3-qubit case. More interestingly, the boundary beyond which there is a violation for the two cases (3-qubit case and 4-qubit case) is the same [31]. Four qubit W states, on the other hand, do not violate the 4-qubit Bell parameter M_4 as measured by Svetlichny's inequality. This is a surprising difference from the behavior of 3-qubit W states which do violate the Svetlichny inequality for some parameters. W states do, however, violate certain other Bell-type inequalities [34, 35].

Based on the past studies of 2-qubits, it was widely thought that entanglement and non-locality are two sides of the same coin and are simply related. Our results show that this is not the case for the multiqubit case, and we provide new insight into the behavior of important classes of multiqubit states. Whereas all entangled states will violate some Bell inequality, their behavior in tests of genuine multiqubit non-locality is not so simple. The criteria for a given entangled state to violate a multipartite Bell test are not well established and our studies are a first step towards developing a general understanding of non-locality in multi-qubit states.

In future, it would be interesting to investigate the N-qubit GGHZ, MS, and W states and test their non-locality properties via an N-qubit Bell inequality [34, 38, 39, 40, 41, 42, 43, 44]. This is interesting because we are exploring one of the greatest mysteries of Nature: quantum correlations across space and time. More and more experiments are being performed in this area, and it is one of the most fascinating areas of fundamental physics [45, 46, 47, 48]. The goal of studying entanglement and quantum non-locality is also to investigate what interesting quantum information tasks multiqubit correlations in GHZ, MS, and W states can be used for. The differences in non-locality

and entanglement between the different classes of states may lead to different possible applications for information processing. We can perhaps execute tasks that are otherwise difficult or impossible and open up new prospects in the future for developing multipartite quantum networks [49], perfect teleportation [42], and superdense coding [42, 50].

Characterization and control of quantum non-locality can thus lead to new technologies in the field of quantum information science that can overcome performance barriers faced by traditional approaches. In other words, it may be possible to perform certain communication tasks in a fundamentally new and faster way. This could eventually reach the status of a commercial application [51]. But even if it does not, the study of quantum correlations remains of fundamental importance to investigate the differences between a universe that is governed by classical laws and the one that we are living in.

Appendix

1. **Matlab code to calculate nonlocality of 2 qubit.**

```
%define variables
m=0;
thetaqmax=0;% angles
thetasmax=0;
phiqmax=0;
phismax=0;
thetarmax=0;
thetatmax=0;
phirmax=0;
phitmax=0;
%
step = 0.3;
for thetaq=(0:step:2)*pi
for thetas=(0:step:2)*pi
for phiq=(0:step:2)*pi
for phis=(0:step:2)*pi
for thetar=(0:step:2)*pi
for thetat=(0:step:2)*pi
for phir=(0:step:2)*pi
for phit=(0:step:2)*pi
y1=-(cos(thetaq)*cos(thetas))-(sin(thetaq)*sin(thetas)*sin(phiq)*sin(phis))-
(cos(phiq)*cos(phis)*sin(thetaq)*sin(thetas));
y2=-(cos(thetar)*cos(thetas))-(sin(thetar)*sin(thetas)*sin(phir)*sin(phis))-
(cos(phir)*cos(phis)*sin(thetar)*sin(thetas));
```

```
y3=-(cos(thetar)*cos(thetat))-(sin(thetar)*sin(thetat)*sin(phir)*sin(phit))-
(cos(phir)*cos(phit)*sin(thetar)*sin(thetat));
y4=-(cos(thetaq)*cos(thetat))-(sin(thetaq)*sin(thetat)*sin(phiq)*sin(phit))-
(cos(phiq)*cos(phit)*sin(thetaq)*sin(thetat));
f = y1 + y2 + y3 - y4;
if f>m
  m=f;
    thetaqmax=thetaq;
    thetasmax=thetas;
    phiqmax=phiq;
    phismax=phis;
    thetarmax=thetar;
    thetatmax=thetat;
    phirmax=phir;
    phitmax=phit;
    end
 %display (f);
end
end
end
end
end
end
end
end
m
thetaqmax
thetasmax
phiqmax
phismax
thetarmax thetatmax phirmax phitmax
```

2. *Matlab code to calculate nonlocality of 3 qubits (GHZ)*

Function file

```
function f= GHZsb2(x,a,b,c)
%a=.5;
%b=0;
%c=sqrt(1-a*a-b*b);
c1 =cos(x(1))*(cos(x(5))*(cos(x(9))+cos(x(11)))+cos(x(7))*(cos(x(9))-cos(x(11))))+
   cos(x(3))*(cos(x(5))*(cos(x(9))-cos(x(11)))-cos(x(7))*(cos(x(9))+cos(x(11))));
c2=sin(x(1))*(sin(x(5))*cos(x(2)+x(6))*(cos(x(9))+cos(x(11)))+sin(x(7))*cos(x(2)+x(8))*
(cos(x(9))-cos(x(11))))+sin(x(3))*(sin(x(5))*cos(x(4)+x(6))*(cos(x(9))-cos(x(11)))-
sin(x(7))*cos(x(4)+x(8))*(cos(x(9))+cos(x(11))));
c3=sin(x(1))*(sin(x(5))*(sin(x(9))*cos(x(2)+x(6)+x(10))+sin(x(11))*cos(x(2)+x(6)+x(12)))
+sin(x(7))*(sin(x(9))*cos(x(2)+x(8)+x(10))-
sin(x(11))*cos(x(2)+x(8)+x(12))))+sin(x(3))*(sin(x(5))*(sin(x(9))*cos(x(4)+x(6)+x(10))-
sin(x(11))*cos(x(4)+x(6)+x(12)))
-sin(x(7))*(sin(x(9))*cos(x(4)+x(8)+x(10))+sin(x(11))*cos(x(4)+x(8)+x(12))));
c4=cos(x(1))*(cos(x(5))*(sin(x(9))*cos(x(10))+sin(x(11))*cos(x(12)))+cos(x(7))*(sin(x(9))*
cos(x(10))-sin(x(11))*cos(x(12))))+cos(x(3))*(cos(x(5))*(sin(x(9))*cos(x(10))-
sin(x(11))*cos(x(12)))-cos(x(7))*(sin(x(9))*cos(x(10))+sin(x(11))*cos(x(12))));
A1=(a^2+b^2-c^2);
A2=2*a*b;
A3=2*a*c;
A4=2*b*c;
f1=A1*c1+A2*c2+A3*c3+A4*c4;
f=-(f1^2);
```

Main file

```
clear
close
clc
%x=[x(1),x(2),x(3),x(4),x(5),x(6),x(7),x(8),x(9),x(10),x(11),x(12)]; % angles;
```

```matlab
lb=[0,0,0,0,0,0,0,0,0,0,0,0];%lower bound
ub=[pi,2*pi,pi,2*pi,pi,2*pi,pi,2*pi,pi,2*pi,pi,2*pi];%upper bound
options=optimoptions(@fmincon,'TolX',10^-
12,'MaxIter',1500,'MaxFunEvals',10^8,'Algorithm','sqp','TolFun',10^-8);
a=0:0.001:1;
b=0.2;
w=NaN(size(a));
ww=NaN(size(a));
for k=1:50 % for loop for the initial value.
  x0=rand([1,12]).*ub*.9986;
for i=1:length(a)
chelp=1-(a(i)^2)-(b^2);% normalized condition
if (chelp>0 || chelp==0)%if statement
  c=sqrt(chelp);
    [~,fval]=fmincon(@(x)GHZsb2(x,a(i),b,c),x0,[],[],[],[],lb,ub,[],options);
w(i)=sqrt(-fval);
else
  w(i)=nan;
end
ww=max(w,ww);
end
end
%h=b.^2;
y=a.^2;
plot(y,ww)
grid on
ylabel('\fontname{Times New Roman} S_{max}(\Psi_{G})')
xlabel('\fontname{Times New Roman}\alpha^2')
```

3. Matlab code to calculate nonlocality of 4-qubits (GHZ)

Function file

```
function f=GHZ4qubit(x,a,b)
%a=.707;
%b=sqrt(1-a*a);
d1=cos(x(1))*(cos(x(5))*(cos(x(9))*(cos(x(13))-cos(x(15)))-
cos(x(11))*(cos(x(13))+cos(x(15))))+cos(x(7))*(cos(x(11))*(cos(x(15))-cos(x(13)))-
cos(x(9))*(cos(x(13))+cos(x(15)))))+
(x(3))*(cos(x(5))*(cos(x(11))*(cos(x(15))-cos(x(13)))-cos(x(9))*(cos(x(13))+cos(x(15))))-
(x(7))*(cos(x(9))*(cos(x(13))-cos(x(15)))-cos(x(11))*(cos(x(13))+cos(x(15))))));
d2=sin(x(1))*(sin(x(5))*(sin(x(9))*(sin(x(13))*cos(x(2)+x(6)+x(10)+x(14))-
sin(x(15))*cos(x(2)+x(6)+x(10)+x(16)))-
sin(x(11))*(sin(x(13))*cos(x(2)+x(6)+x(12)+x(14))+sin(x(15))*cos(x(2)+x(6)+x(12)+x(16))
))+sin(x(7))*(sin(x(11))*(sin(x(15))*cos(x(2)+x(8)+x(12)+x(16))-
sin(x(13))*cos(x(2)+x(8)+x(12)+x(14)))-
sin(x(9))*(sin(x(13))*cos(x(2)+x(8)+x(10)+x(14))+sin(x(15))*cos(x(2)+x(8)+x(10)+x(16))))
)+sin(x(3))*(sin(x(5))*(sin(x(11))*(sin(x(15))*cos(x(4)+x(6)+x(12)+x(16))-
sin(x(13))*cos(x(4)+x(6)+x(12)+x(14)))-
sin(x(9))*(sin(x(13))*cos(x(4)+x(6)+x(10)+x(14))+sin(x(15))*cos(x(4)+x(6)+x(10)+x(16))))
-sin(x(7))*(sin(x(9))*(sin(x(13))*cos(x(4)+x(8)+x(10)+x(14))-
sin(x(15))*cos(x(4)+x(8)+x(10)+x(16)))-
sin(x(11))*(sin(x(13))*cos(x(4)+x(8)+x(12)+x(14))+sin(x(15))*cos(x(4)+x(8)+x(12)+x(16))
)));
A1=2*a*b;
f1=d1+A1*d2;
f=-(f1^2);
```

Main file

```
close
clc
lb=[0,0,0,0,0,0,0,0,0,0,0,0,0,0,0,0];% lower bound
```

```
ub=[pi,2*pi,pi,2*pi,pi,2*pi,pi,2*pi,pi,2*pi,pi,2*pi,pi,2*pi,pi,2*pi];%upper bound
options=optimoptions(@fmincon,'TolX',10^-
12,'MaxIter',1500,'MaxFunEvals',10^8,'Algorithm','sqp','TolFun',10^-8);
a=0:0.001:1;
b=sqrt(.6);
   w=NaN(size(a));
   ww=NaN(size(a));
   for k=1:80
      x0=rand([1,16]).*ub*.9986;
      for i=1:length(a)
         chelp=1-(a(i)^2)-(b^2);
         if (chelp>0 || chelp==0)

c=sqrt(chelp);[~,fval]=fmincon(@(x)GHZ4qubit(x,a(i),b,c),x0,[],[],[],[],lb,ub,[],options);
   w(i)=sqrt(-fval);
         else
               w(i)=nan;
         end
         ww=max(w,ww);
      end
   end
   %yy=b.^2;
   xx=a.^2;
   %FOR BEST looking crossing of lines use smaller a=0:0.001:1;
   figure1 = figure;
   ax1 = axes('Position',[0 0 1 1],'Visible','off');
   ax2 = axes('Position',[.1 .1 .85 .85]);
   ww2=ww-8;
   indexes=find(ww2(1:length(ww2)-1).*ww2(2:length(ww2))<0);
   plot(ax2,xx,ww)
   hold on
```

```
    plot([0 1],[8 8],'color','red','linestyle','--')
  if length(indexes)==2
      hold on
      plot([xx(indexes(1)) xx(indexes(1))],[0 8],'color','red','linestyle','--')
      hold on
      plot([xx(indexes(2)+1) xx(indexes(2)+1)],[0 8],'color','red','linestyle','--')
    %first choice
      axes(ax1) % sets ax1 to current axes
      text(xx(indexes(1))+0.04,0.06,'\fontname{Times New Roman}min \alpha^2')
      axes(ax1) % sets ax1 to current axes
      text(xx(indexes(2))-0.04,0.06,'\fontname{Times New Roman}max \alpha^2')
  end
  %maximize screen to not overlap (values)
  %set(gca, 'XTick', sort([x(indexes(1)), get(gca, 'XTick')]));
  %set(gca, 'XTickLabel', get(gca, 'XTickLabel'));
  %set(gca, 'XTick', sort([x(indexes(2)+1), get(gca, 'XTick')]));
  axes(ax2)
  grid on
  %ylabel('\fontname{Times New Roman} S_{max}(\Psi_{G})')
  %ylabel('\fontname{Times New Roman} S_{max}(\Psi_{W})')
  xlabel('\fontname{Times New Roman}\alpha^2')
  ylabel('\fontname{Times New Roman} M_{max}')
  str1 = {'\beta^2 = 0.6'};
  text(.9,4,str1)
  %title(strcat('\fontname{Times New Roman} Maximum of the Svetlichny operator.
Method 1 (alpha|000>+beta|110>+gamma|111>), b=',num2str(b)))
  %saveas(figure1,strcat(strcat('b=',num2str(b)),'.jpg'))
  %second choice
  % axes(ax1) % sets ax1 to current axes
  % str = 'min alpha';
  % dim = [x(indexes(1)) 0 0 .2];
```

```
% annotation('textbox',dim,'String',str,'FitBoxToText','on');
% dim = [x(indexes(2)) 0 0 .2];
% annotation('textbox',dim,'String',str,'FitBoxToText','on');
%end
```

Bibliography

[1] Demtröder, W. (2006). *Atoms, molecules and photons: an introduction to atomic, molecular and quantum physics.* Germany, Springer.

[2] Newton, R. G. (2013). *Scattering theory of waves and particles*. USA, Springer Science and Business Media.

[3] Loudon, R. (2000). Quantum mechanics of the atom radiation interaction. *The quantum theory of light* (p. 46). OUP. Oxford University Press.

[4] Fermi, E. (1932). Quantum theory of radiation. *Reviews of Modern Physics, 4*(1), 87-123.

[5] Einstein, A., Podolsky, B., & Rosen, N. (1935). Can quantum-mechanical description of physical reality be considered complete?. *Physical Review*, *47*(10), 777-780.

[6] Gisin, N. (2009). Quantum nonlocality: how does nature do it?. *Science, 326*(5958), 1357-1358.

[7] Accardi, L. (1988). Foundations of quantum mechanics: a quantum probabilistic approach. In *The Nature of quantum paradoxes* (pp. 257-323). Springer Netherlands.

[8] Bell, J. S. (1964). On the Einstein Podolsky Rosen paradox. *Physical Review, 1*(3), 195-200.

[9] Bell, J. S. (1966). On the problem of hidden variables in quantum mechanics. *Reviews of Modern Physics*, *38*(3), 447-452.

[10] Bohm, D., & Aharonov, Y. (1957). Discussion of experimental proof for the paradox of Einstein, Rosen, and Podolsky. *Physical Review*, *108*(4), 1070-1076.

[11] Liang, Y. C., Rosset, D., Bancal, J. D., Pütz, G., Barnea, T. J., & Gisin, N. (2015). Family of bell-like inequalities as device-independent witnesses for entanglement depth. *Physical Review Letters*, *114*(19), 190401.

[12] Xiang, Y., & Ren, W. (2011). Joint measurements and Svetlichny's inequality. *Journal of Physics A: Mathematical and Theoretical*, *44*(32), 325305.

[13] Svetlichny, G. (1987). Distinguishing three-body from two-body non-separability by a Bell-type inequality. *Physical Review D*, *35*(10), 3066.

[14] Giuliano, B., Giulio, C., & Giuliano, S. (2004). Quantum Computation. *Principles of quantum computation and information volume I: basic concepts* (pp. 99-112). Singapore, World Scientific.

[15] Nielsen, M. A., & Chuang, I. L. (2010). *Quantum computation and quantum information*. Cambridge university press.

[16] Williams, C. P. (2010). *Explorations in quantum computing*. New York, Springer Verlag.

[17] Arfken, G. B., & Weber, H. J. (2005). *Mathematical methods for physicists (sixth edition)*. USA, Elsevier Academic Press.

[18] Ghose, S. (2009). The Einstein-Podolsky-Rosen paradox and the nature of reality. *Physics in Canada*, *65*(4), 199-204.

[19] Sakurai, J. J., & Napolitano, J. (2011). *Modern quantum mechanics*. San Francisco, CA, Addison Wesley publishing company.

[20] Clauser, J. F., & Shimony, A. (1978). Bell's theorem. Experimental tests and implications. *Reports on Progress in Physics*, *41*(12), 1881-1927.

[21] Freedman, S. J., & Clauser, J. F. (1972). Experimental test of local hidden-variable theories. *Physical Review Letters*, *28*(14), 938-941.

[22] Fry, E. S., & Thompson, R. C. (1976). Experimental test of local hidden-variable theories. *Physical Review Letters*, *37*(8), 465-468.

[23] Tapster, P. R., Rarity, J. G., & Owens, P. C. M. (1994). Violation of Bell's inequality over 4 km of optical fiber. *Physical Review Letters*, *73*(14), 1923-1926.

[24] Kwiat, P. G., Mattle, K., Weinfurter, H., Zeilinger, A., Sergienko, A. V., & Shih, Y. (1995). New high-intensity source of polarization-entangled photon pairs. *Physical Review Letters*, *75*(24), 4337-4341.

[25] Tittel, W., Brendel, J., Zbinden, H., & Gisin, N. (1998). Violation of Bell inequalities by photons more than 10 km apart. *Physical Review Letters*, *81*(17), 3563-3566.

[26] Weihs, G., Jennewein, T., Simon, C., Weinfurter, H., & Zeilinger, A. (1998). Violation of Bell's inequality under strict Einstein locality conditions. *Physical Review Letters*, *81*(23), 5039-5043.

[27] Aspect, A. (1999). Bell's inequality test: more ideal than ever. *Nature*, *398*(6724), 189-190.

[28] Ou, Z. Y., & Mandel, L. (1988). Violation of Bell's inequality and classical probability in a two-photon correlation experiment. *Physical Review Letters*, *61*(1), 50-53.

[29] Shih, Y. H., & Alley, C. O. (1988). New type of Einstein-Podolsky-Rosen-Bohm experiment using pairs of light quanta produced by optical parametric down conversion. *Physical Review Letters*, *61*(26), 2921-2924.

[30] Neeley, M., Bialczak, R. C., Lenander, M., Lucero, E., Mariantoni, M., O'Connell, A. D., ... & Yin, Y. (2010). Generation of three-qubit entangled states using superconducting phase qubits. *Nature*, *467*(7315), 570-573.

[31] Ghose, S., Debnath, S., Sinclair, N., Kabra, A. A., & Stock, R. (2010). Multiqubit nonlocality in families of 3-and 4-qubit entangled states. *Journal of Physics A: Mathematical and Theoretical*, *43*(44), 445301.

[32] Ajoy, A., & Rungta, P. (2010). Svetlichny's inequality and genuine tripartite nonlocality in three-qubit pure states. *Physical Review A*, *81*(5), 052334.

[33] Cereceda, J. (2002). 3-particle entanglement versus 3-particle non-locality. *Physical Review A, 66*(2), 28038.

[34] Wu, C., Chen, J. L., Kwek, L. C., & Oh, C. H. (2006). Quantum nonlocality of N-qubit W states. *Physical Review A*, *73*(1), 012310.

[35] Ding, D., Yan, F., & Gao, T. (2013). Bell-type inequality and quantum nonlocality in four-qubit systems. *arXiv preprint arXiv:1310.6300*.

[36] Clauser, J. F., Horne, M. A., Shimony, A., & Holt, R. A. (1969). Proposed experiment to test local hidden-variable theories. *Physical Review Letters*, *23*(15), 880.

[37] Gisin, N. (1991). Bell's inequality holds for all non-product states. *Physics Letters A*, *154*(5-6), 201-202.

[38] Hu, M. L. (2011). Robustness of Greenberger–Horne–Zeilinger and W states for teleportation in external environments. *Physics Letters A*, *375*(5), 922-926.

[39] Collins, D., Gisin, N., Popescu, S., Roberts, D., & Scarani, V. (2002). Bell-type inequalities to detect true n-body nonseparability. *Physical Review Letters*, *88*(17), 170405.

[40] Chaves, R., Acín, A., Aolita, L., & Cavalcanti, D. (2014). Detecting nonlocality of noisy multipartite states with the Clauser-Horne-Shimony-Holt inequality. *Physical Review A*, *89*(4), 042106.

[41] Seevinck, M., & Svetlichny, G. (2002). Bell-type inequalities for partial separability in N-particle systems and quantum mechanical violations. *Physical Review Letters*, *89*(6), 060401.

[42] Agrawal, P., & Pati, A. (2006). Perfect teleportation and superdense coding with W states. *Physical Review A*, *74*(6), 062320.

[43] Parashar, P., & Rana, S. (2009). N-qubit W states are determined by their bipartite marginals. *Physical Review A*, *80*(1), 012319.

[44] Sen, A., Sen, U., Wieśniak, M., Kaszlikowski, D., & Żukowski, M. (2003). Multiqubit W states lead to stronger nonclassicality than Greenberger-Horne-Zeilinger states. *Physical Review A*, *68*(6), 062306.

[45] Thaheld, F. (2003). Biological nonlocality and the mind–brain interaction problem: comments on a new empirical approach. *BioSystems*, *70*(1), 35-41.

[46] Hensen, B., Bernien, H., Dréau, A. E., Reiserer, A., Kalb, N., Blok, M. S., ... & Amaya, W. (2015). Experimental loophole-free violation of a Bell inequality using entangled electron spins separated by 1.3 km. *Nature*, *526*, 682-686.

[47] Giustina, M., Versteegh, M. A., Wengerowsky, S., Handsteiner, J., Hochrainer, A., Phelan, K., ... & Amaya, W. (2015). Significant-loophole-free test of Bell's theorem with entangled photons. *Physical Review Letters*, *115*(25), 250401.

[48] Shalm, L. K., Meyer-Scott, E., Christensen, B. G., Bierhorst, P., Wayne, M. A., Stevens, M. J., ... & Coakley, K. J. (2015). Strong loophole-free test of local realism. *Physical Review Letters*, *115*(25), 250402.

[49] Cavalcanti, D., Skrzypczyk, P., Aguilar, G. H., Nery, R. V., Ribeiro, P. S., & Walborn, S. P. (2015). Detection of entanglement in asymmetric quantum networks and multipartite quantum steering. *Nature Communications*, *6*, 7941.

[50] Saha, D., & Panigrahi, P. K. (2012). N-qubit quantum teleportation, information splitting and superdense coding through the composite GHZ–Bell channel. *Quantum Information Processing*, *11*(2), 615-628.

[51] Gruska, J. (2007). A broader view on the limitations of information processing and communication by nature. *Natural Computing*, *6*(2), 75-112.